FOI-R--1579--SE
February 2005
ISSN 1650-1942
Technical report

Jörgen Carlsson

Flame spread and fire growth –

Modelling capabilities in various room configurations

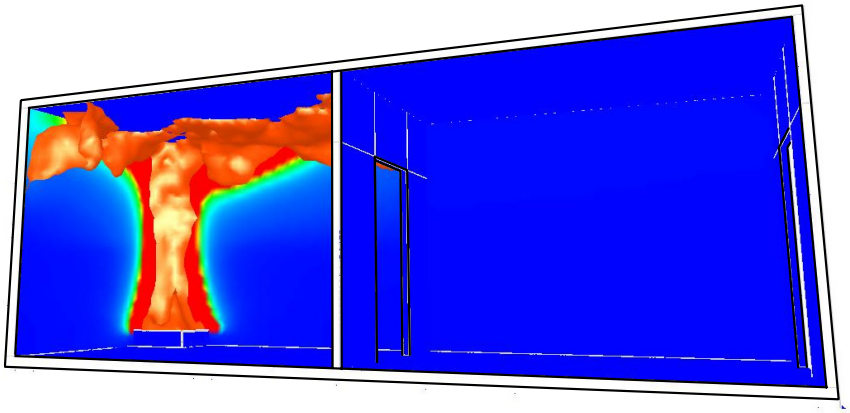

Weapons and Protection
SE-147 25 Tumba

SWEDISH DEFENCE RESEARCH AGENCY
Weapons and Protection
SE-147 25 Tumba

FOI-R--1579--SE
February 2005
ISSN 1650-1942
Technical report

Jörgen Carlsson

Flame spread and fire growth –

Modelling capabilities in various room configurations

Cover:
Snapshot from a flame spread simulation using FDS2 created in the visualisation tool Smokeview

Issuing organization	Report number, ISRN	Report type
FOI – Swedish Defence Research Agency Weapons and Protection SE-147 25 Tumba	FOI-R--1579--SE	Technical report
	Research area code 5. Combat	
	Month year February 2005	**Project no.** E2353
	Customers code 5. Commissioned Research	
	Sub area code 53 Protection and Fortification	

Author/s (editor/s)	
Jörgen Carlsson	**Project manager** Jörgen Carlsson
	Approved by Rickard Forsén
	Sponsoring agency Armed Forces
	Scientifically and technically responsible Jörgen Carlsson

Report title

Flame spread and fire growth – Modelling capabilities in various room configurations

Abstract (not more than 200 words)

During 2002 and 2003 a series of experimental studies in model-scale were performed to investigate compartment flame spread and fire growth in compartments and fire spread between compartments. The extensive library of measurement data was used in evaluating the flame-spread modelling capabilities of the popular CFD code FDS.

Input data to the material model was derived using an iterative approach, comparing stand alone predictions with experimental data on surface temperature and mass loss rate obtained from different external heat fluxes. The initial side length of the computational grid was chosen related to the dimensionless initial fire size. This choice proved to be optimal in terms of numerical agreement with the experimental data on parameters such as gas temperature, velocity and fire growth rate. Furthermore, this was shown to hold in all the tested configurations. Strictly speaking, a numerical simulation must show identical results regardless of timestep and meshing but no grid independence could be obtained, making any arbitrary simulation difficult to interpret unless the results are known beforehand.

The mechanism of thermal degradation of a combustible material is rather well investigated and documented. From a flame-spread modelling point of view the modelling of the convective and the radiative heat fluxes need further research and development.

Keywords

Ignition, fire, pyrolysis, fire growth, flame spread, flashover, CFD, modelling

Further bibliographic information	Language English
ISSN 1650-1942	**Pages** 63 p.
	Price acc. to pricelist

Utgivare	Rapportnummer, ISRN	Klassificering
Totalförsvarets Forskningsinstitut - FOI	FOI-R--1579--SE	Teknisk rapport
Vapen och skydd	**Forskningsområde**	
147 25 Tumba	5. Bekämpning	
	Månad, år	**Projektnummer**
	Februari 2005	E2353
	Verksamhetsgren	
	5. Uppdragsfinansierad verksamhet	
	Delområde	
	53 Skydd och anläggningsteknik	

Författare/redaktör	Projektledare
Jörgen Carlsson	Jörgen Carlsson
	Godkänd av
	Rickard Forsén
	Uppdragsgivare/kundbeteckning
	Försvarsmakten
	Tekniskt och/eller vetenskapligt ansvarig
	Jörgen Carlsson

Rapportens titel (i översättning)

Flamspridning och brandtillväxt - En modellutvärdering i olika rumskonfigurationer

Sammanfattning (högst 200 ord)

Vid FOI genomfördes under 2002 och 2003 en omfattande modellskalestudie av flamspridning och brandtillväxt i olika rumskonfigurationer. Det här projektet har dragit nytta av det befintliga experimentella underlaget i ett försök att utvärdera flamspridningsmöjligheterna i CFD koden FDS.

För att härleda indata till pyrolysmodellen användes experimentella data från olika antändningsförsök där yttemperaturen registrerats löpande. Genom att lösa dels värmeledningsekvationen dels pyrolysmodellen med successivt ändrade indatavärden identifierades en uppsättning indata för det aktuella materialet. Storleken på beräkningsgriden valdes som en första approximation som en fraktion av den dimensionslösa diametern på initialbrandkällan. Detta visade sig vara det val som genomgående gav bäst resultat. Gridoberoende kunde emellertid inte erhållas varför de initialt goda resultaten, i strikt mening, inte är så mycket värda då det experimentella utfallet måste vara känt i förväg för att några definitiva slutsatser ska kunna dras.

Termisk nedbrytning av ett material har studerats i flera decennier och de grundläggande mekanismerna är relativt väl dokumenterade. Problemet som identifieras i denna rapport har sin grund i de förenklade modellerna för värmeöverföring från en varm gasmassa till en brännbar yta.

Nyckelord

Antändning, brand, pyrolys, brandtillväxt, brandspridning, övertändning, CFD, brandmodellering

Övriga bibliografiska uppgifter	Språk Engelska
ISSN 1650-1942	**Antal sidor:** 63 s.
Distribution enligt missiv	**Pris: Enligt prislista**

Table of contents

Nomenclature

Below, attention is briefly directed at a number of basic terms and concepts used within the report.

Firstly the term “flame spread model” refers to all the submodels for the calculation of fluid flow, combustion and different heat transfer mechanisms, as well as routines for modelling the thermal decomposition of the solid material. The latter is generally referred to as a material- or a pyrolysis model.

The following nomenclature has been employed:

c_p	specific heat capacity at constant pressure,
g	gravity (9.8 m/s^2)
h	specific enthalpy or heat transfer coefficient,
k	thermal conductivity,
k_a	gas absorption coefficient,
m	mass,
q	heat release per unit mass
t	time,
U *or* $\boldsymbol{u}$	velocity vector,

A	Arrhenius pre-exponential factor for a chemical reaction or area,
E_a	activation energy,
ΔH_c	heat of combustion,
ΔH_{ev}	heat of combustion,
ΔH_{py}	heat of evaporation,
HRR	heat release rate, dQ/dt,
I	radiant intensity,
I_b	black body intensity,
Pr	Prandtls number,
Q	heat release,
R	gas constant,
T	temperature,

δ	thickness,
ε	emissivity,
Γ	diffusivity,
ν	kinematic viscosity,
ρ	density,
χ	radiative fraction,
ϕ	symbol for an arbitrarily scalar,
Ω	arbitrarily volume in space,

Superscripts

’’	per unit area,
’’’	per unit volume,
·	time derivative,

Subscripts

0	ambient or initial value,
a	active material,

i, j, k	cartesian co-ordinator directions,
loc	local value
m	moisture,
py	pyrolysis,
w	wood,
∞	infinity,

1. Introduction

Simulation of fire and fire induced phenomena is a challenging field of research. It involves the modelling of a turbulent, buoyancy driven and chemically reacting flow and its effects on the surroundings. Until recently, limitations set by computational resources put a serious constraint on any modelling effort based on first principles. Instead, semi-empirical models, often developed for specific end-use scenarios was developed and used in studies concerning smoke movement, temperature development due to fire and even flame spread and fire growth. With the advance in computer power it became practicable, at least to some degree, to make better use of first principles in fire calculations. At this time, say in the late 80's, CFD, basically referring to a set of numerical procedures used to solve the computationally demanding partial differential equations describing fluid motion, had been used in many different engineering disciplines and was now also embraced by the fire researchers.

Writing 2004 it is now possible, given proper care, to use existing CFD software to solve for the transient smoke movement along with its temperature distribution in space in rather arbitrarily geometries. But many problems remain, one of these being the prediction of heat transfer from the fluid (gas) to the surfaces of a solid material, such as a wall or a ceiling. This is unfortunate since the heat flux governs ignition and the subsequent spread of flame on the surface of a material such as a combustible lining, thus governing the fire growth.

1.1 Background

During 2001 and 2002, a number of ignition experiments were carried out at FOI, the Swedish Defence Research Agency, using a pulsating CO_2 laser as heating source[1,2]. The sample surface temperature was recorded using thermocouple measurements and an IR-equipment, the time to ignition was also monitored visually. Furthermore, in 2003, a series of experiments were carried out studying the transient fire growth in one and two room configurations.[3] The analysis included the effects of ventilation and the means of fire initiation. The compartments were, fully or partially, lined with medium density fibreboards, MDF, allowing flame-spread within, and between, the compartments to be evaluated. Several important issues were highlighted from the experiments. The commonly accepted criterion for flashover, 20 kW/m^2, to floor was shown to be on the unsafe side rather than being a conservative approximation. Another common critical limit for flashover based on the average temperature of fire gases was however, confirmed. Furthermore, the time to ignition was shown to be closely linked to the mode of initiation and initial fuel type.

Many researchers and code developers have claimed that their software provide the means to model fire growth in room fires. Indeed, this would be a desirable feature in assessing

building fire safety since the course of fire development would not have to be approximated through engineering methods but evaluated depending on the combustible materials being present in the compartments of interest. However, recent studies have shown that the flame spread problem is still unsolved for all but the simplest scenarios for which several models can be tuned to provide qualitative results and to some extent produce reasonable quantitative predictions[4]. At this point, no flame-spread model has been proven a reliable tool to the fire safety engineering community.

1.2 Purpose and objective

A theoretical response to any experimental test program is fundamental in order to extract the core of information being held within the measured test data. Therefore, the purpose of this study is to fill in some missing pieces, trying to find answers to some of the questions which arise from recent experimental work performed by the Fire Technology Group at FOI. The report aims at a comprehensive review of the flame spread phenomena from gas phase modelling, heat transfer to and through a solid leading to ignition, the pyrolysis process and the subsequent flame spread and fire growth. This will lead to an understanding of the possibilities and limitations of different models involved in the simulation, including the ones used in deriving input data, thus allowing an identification of problem areas which need additional attention.

While surface flame spread on interior wooden walls may not be a very high priority from a military perspective, the scenario being more interesting to architects, designers and safety engineers, the course of events associated with such a fire scenario, starting with fire initiation followed by fire growth and a subsequent flashover and ventilation controlled burning is, however, of major importance in evaluating the fire safety in most military applications. This work is concerned with fire initiation by “normal” events such as electrical failure, fuel leakage and the like. Extremely high, short duration, heat fluxes arising from direct weapons induced phenomena are not covered.

1.3 Overview of the report

Chapter 2 will give a short summary of some related ongoing or recently presented research in the field of heat transfer from flames, ignition and flame spread putting the work performed within the framework of this project into perspective.

The following chapter, Chapter 3, presents the experimental basis for this theoretical review. It includes a short review of the Cone Calorimeter, ISO 5660, for ignition and heat release

measurements, highlighting some of its weaknesses. Furthermore, surface temperature measurements using different measurement techniques are presented. Finally the model-scale flame-spread and fire growth experiments are summarised.

Chapter 4 gives a brief introduction to gas phase modelling including the turbulent combustion but with the emphasis on the modelling of the radiative and the convective heat transfer to a solid boundary as implemented in the CFD code FDS.

The thermal response of a combustible material to a heat exposure is characterised by the rate of generation of combustible pyrolysis gases. Chapter 5 presents the pyrolytic process describing the thermal degradation of wood. The difficulties introduced are not unique for wood but applies to several practical building materials. Furthermore, the pyrolysis model implemented into version 2 of FDS is presented to be used later in the report.

In Chapter 6 the test data obtained from the experiments described in Chapter 3 is used to derive input data to the pyrolysis model. A systematic methodology is presented and some different techniques are compared.

Chapter 7 presents results from using the flame spread model to predict the fire growth in experiments of one and two room configurations. Experimental data from fire heat release rate, gas temperature and velocities are compared with model predictions. Furthermore, a simple analytical relationship is described and evaluated in short.

2. Some related research

In the late 1960's John de Ris[6] pioneered the theoretical analysis of flame spread in his work on the spread of laminar diffusion flames. In the decades that followed the governing equations were described in some detail including momentum, heat and mass transfer in the solid material. However, since the hot, fire induced, flow could not be adequately described researchers tried to approximate the spread of flame using analytical equations tuned for specific end use scenarios. This work was influenced by Williams[7] who qualitatively described different modes of flame spread using a relationship that he named "the fundamental equation of flame spread", Equation 1. He encouraged the use of a practical methodology where all but the most important features were ignored, thus putting the focus on important but yet unsolved key phenomena and in the end obtaining a solvable set of equations.

$$u_{py} \propto \frac{\dot{q}}{\rho \Delta h} \qquad \text{Eq. 1}$$

The fundamental equation of flame spread summarises the theory of the flame spread phenomena stating that the spread rate, referring to the velocity of the pyrolysis front, is governed by the incident net heat flux divided by the material density and the enthalpy.

Following the growing interest on performance based fire safety design some researchers worked to find a flame spread model that could be used as an engineering tool. Among those were Thomas and Karlsson[8] who found a way of solving the flame spread equation derived by Saito, Quintiere and Williams[9], ending up with a set of complementary analytical equations. Shortly thereafter, Karlsson[10] presented a methodology to use the model equations obtaining good agreement with experimental data in a one compartment scenario including a variety of combustible materials. It was shown that the model could be used in estimating the fire growth in scenarios with, and without, combustible linings attached to the ceiling. Despite the successful sample calculations, the flexibility of this kind of model is, however, very low.

A few years later, computers had become sufficiently fast to allow the solution of a simplified set of governing equations for the turbulent reacting flow. Yan[11] was among those who first explored the possibility to couple different pyrolysis models to the general solution of the flow field using computational fluid dynamics, CFD. A first attempt using data directly from the small scale test apparatus, the Cone Calorimeter, was deemed as moderately successful thus Yan developed a pyrolysis model based on the heat transfer through the solid material. The results were promising and several researchers followed, basically using the same model equations. The pyrolysis model proposed by Yan is still being used by different researchers coupled to CFD codes using different submodels.

Hostikka and McGrattan[12] implemented the pyrolysis model of Atreya[13], based on a first order Arrhenius rate reaction equation, into the popular CFD code FDS. This is the combination used for calculations in this study and will be described in more detail in the following chapters. The approach is promising but the details, concerning the pyrolytic behaviour as well as the fluid dynamics, are yet to be perfected. This is a general problem in flame spread modelling and has been recognised by a group of researchers under the supervision of Prof Holmstedt in the CECOST group (The Centre for Combustion Science and Technology)[14] who, basically following the advice of Williams, approach the problem systematically adding details as they become well understood. Their work have focused on detailed measurements of kinetic parameters and the processes governing pyrolysis, they also study the heat transfer in the interface between the gas phase and the solid material as well as measurement of surface temperature using a thermographic phosphors technique.

3. Experimental methods

Input data to any pyrolysis model include the thermal properties of the solid as well as parameters governing ignition and the subsequent thermal response of the combustible material. These parameters are, as a rule, rather difficult to find in the literature. Unambiguous and validated kinetic data are scarce and may differ by several orders of magnitude for the same material. The reason for this may be attributed to different measurement techniques. Model simplifications add to the difficulties as model developers tend to include unknown, or unresolved, physics into any available parameter, which may then make literature data on the physical parameter inadequate.

The solution to this discrepancy between model and reality has been to use small scale experiments, most often the Cone Calorimeter, choosing input data according to a best-fit analysis, comparing model predictions with measured results on mass loss rate and time to ignition for different incident heat fluxes until a set of parameters providing a satisfactory comparison has been identified. This chapter will give a short description of the different experimental setups used to derive the input parameters to the pyrolysis model. Furthermore, the model-scale experiments are summarised.

3.1 Evaluation of ignition using a CO_2 laser source

In order to evaluate the onset of ignition at different heat fluxes Walmerdahl[1,2] used a pulsating CO_2 laser as a heat source reaching an incident heat flux as high as 190 kW/m^2. The sample material was a 9 mm thick MDF board, its centre being exposed to a laser beam with a diameter of 3 cm. The intensity distribution of the beam was controlled using beam expanders making the exposure uniform. Both spontaneous and piloted ignition was considered. The test series with piloted ignition used a cantal wire to initiate a combustion reaction in the pyrolysis gases. During the tests a number of measurements were recorded including rate of pyrolysis (mass loss), surface temperature and time to ignition. The setup is presented in Figure 1.

Despite the rather good repeatability that was shown it can be expected that the method suffers from sensitiveness of boundary conditions and scale effects. At this time, no experimental data exists where this has been evaluated.

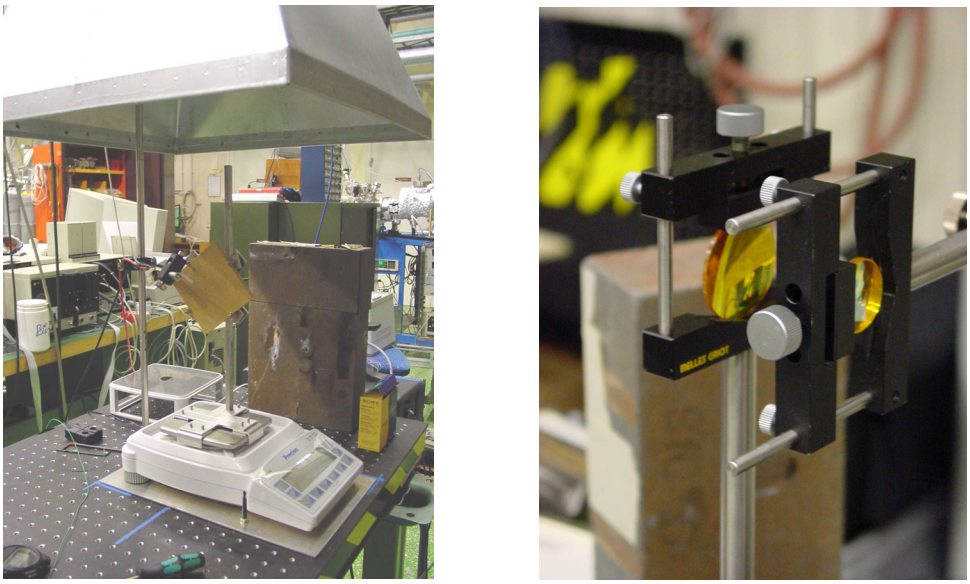

Figure 1. Sample holder, scale and exhaust hood (left) and beam expanders (right). From reference 2.

3.2 The Cone Calorimeter

The Cone Calorimeter, shown schematically in Figure 2, has been used for classification purposes for a long time and it is widely spread. The method is standardised and has been proven to provide results that are repeatable and reproducible. Although frequently used by modellers, the results from this testing apparatus was never intended to be used for model development, model validation or to derive input data to model equations, the reason for its continuing use by modellers being the lack of alternatives. Complete information on the Cone Calorimeter can be readily found from several sources[5,10,15] and in the following only a few of the major drawbacks using the method for model development and evaluation purposes will be repeated in brief.

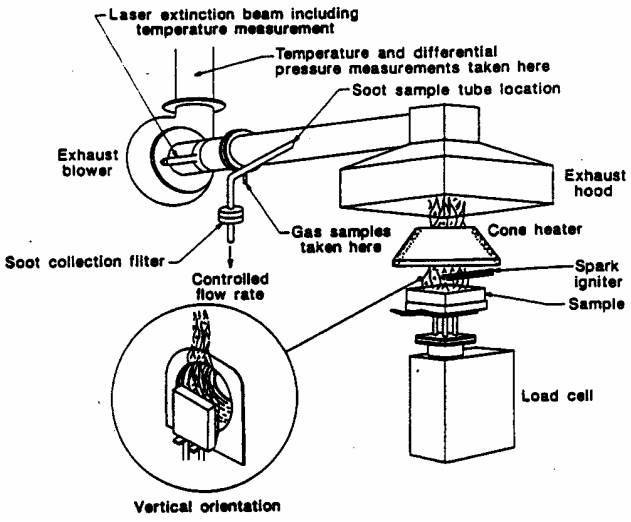

Figure 2. Sketch of the Cone Calorimeter. From reference 10.

Even though the standard is sufficiently detailed to enable a high level of repeatability to be achieved, one should bear in mind the different factors that can affect the outcome of a test and of a simulation based upon the experimental results. One such factor is the physical scale of the sample tested. The standard size of the specimen is 0.1×0.1 meters. In examining different materials in a modified Cone Calorimeter, using samples of the dimensions 0.2×0.2 meters (corresponding to a surface area four times as large as the original being exposed), however, Nussbaum and Östman[16] concluded that some materials which failed to ignite in the original test, such as the melamine-faced particleboard at 25 kW/m^2, for example, indeed did ignite when the sample area was increased. The time to ignition was typically found to differ by about 20%, but for wooden materials such as spruce panel or particleboard the discrepancy was closer to 30%. The peak heat release rate per unit area for the wooden materials was shown to be about 20% higher for the larger samples, while the one-minute average heat release rate differed by less then 10%. The results presented by Nussbaum and Östman has been corroborated by Babrauskas[17], referring to tests on PMMA carried out at Factory Mutual.

Another factor that may be of great importance to the modeller is the orientation of the sample. The usual procedure is to keep the sample in a horizontal position, face up, during testing. This is in contrast with what would normally be modelled, such as a vertical wall or a lining under ceiling (combustible material facing down). The effects of sample orientation are exemplified in Figure 3 presenting results of experiments on Radiata pine performed by Moghtaderi[18].

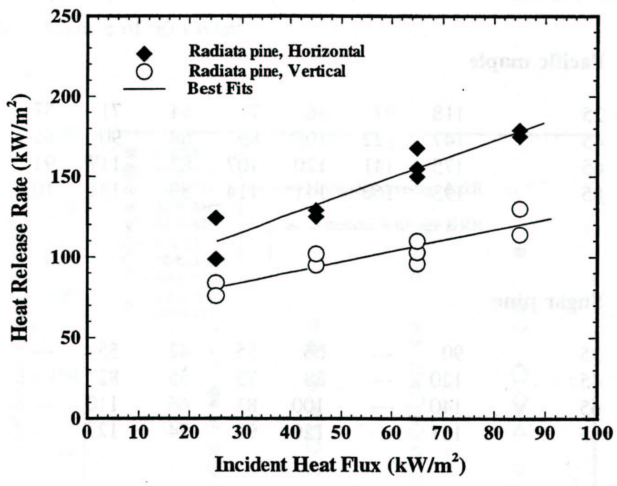

Figure 3. Differences between horisontal and vertical orientation during a test in the Cone Calorimeter. From reference 18.

For wooden materials, the typical transient heat release curve the Cone Calorimeter provides consists of two peaks. The first peak can be expected under any circumstances when wood or any other charring materials are burning, although its appearance may differ somewhat from one test to another, depending on the sampling interval involved. The presence of this first

peak can be explained based on an insulating carbonaceous char layer being formed, creating a protecting coat in front of the yet unburned wood and leading to a rapid decrease in the heat release rate after the first peak. The presence of the second peak indicates the thermal wave to have reached the insulated back side of the sample and heat to have accumulated at the insulated rear end of it, enhancing pyrolysis and increasing the rate of heat release. Thus, the second peak is artificial in a sense, and is highly dependent upon the character of the backing material. This has been studied by Tsantaridis[19], his results showing the effect of sample thickness is illustrated in Figure 4.

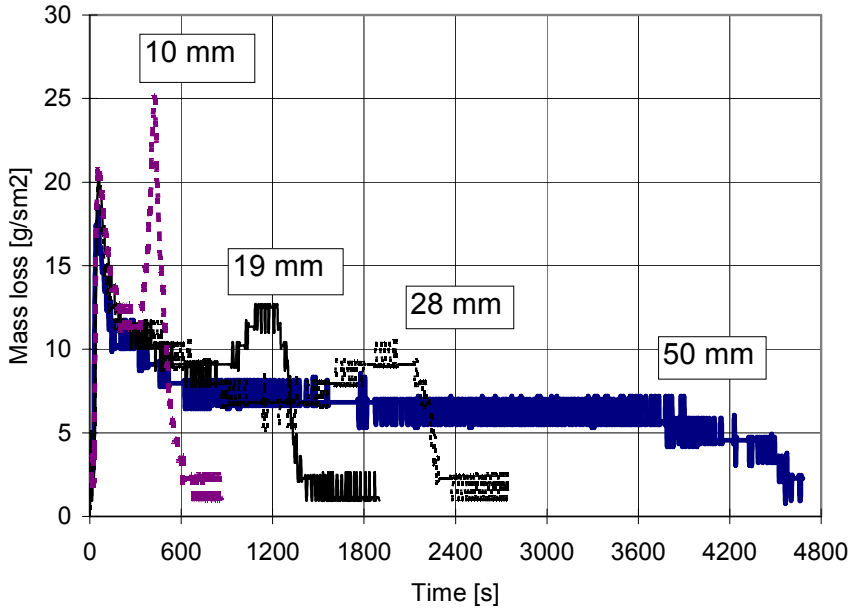

Figure 4. Effects of the backing conditions during tests with a horizontal orientation. From reference 19.

Furthermore, no experimental data have been found relating to the increase in the incident heat flux due to flaming combustion affecting the sample after onset of ignition. In a simulation studying the flame heat flux using a RANS based CFD code, Carlsson[4] showed a significant variation in heat feedback over the sample, with a peak in the centre and a considerable decrease towards the edges. Furthermore, it is evident that the heat feedback changes during testing because of the varying heat release rate and the following variation in flame depth and emissivity.

3.3 Fire growth and flame spread tests in model scale

During 2003 a series of model scale tests studying flame spread and fire growth in different room configurations were carried out at FOI[3]. The initial tests, using a single compartment with combustible linings on its walls, the door-wall excluded, and under the ceiling, were aiming at understanding the influence of the ignition source on fire development and time to

flashover. In the following tests a second compartment was attached to the primary fire compartment in an investigation of vertical and horizontal room-to-room flame spread. Interior surfaces were completely or partially lined with MFD board. To investigate the effect of different ventilation conditions the size of the openings between compartments and between compartments and the outside were varied.

A side-view diagram of the different room configurations showing its inner dimensions in mm are presented in Figure 5 below.

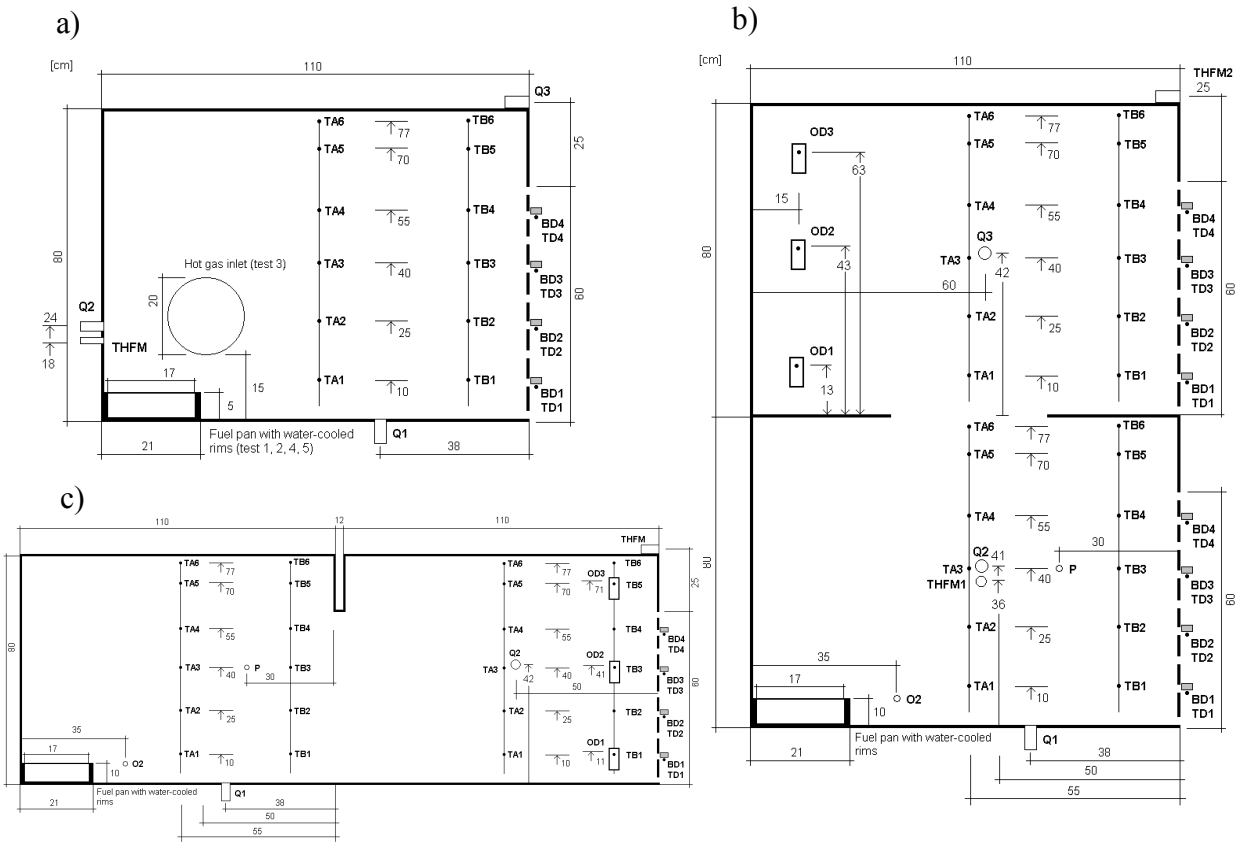

Figure 5. Sketch of the enclosures in the configurations used in the flame spread tests, a) shows the original module, the opening dimensions are kept constant during single compartment tests, b) example of experimental rig from vertical flame-spread tests and c) horizontal flame-spread test. From reference 3.

The measurements included those of the gas flow characteristics in a hood, required for the heat release rate evaluation and of the mass loss rate of the initial source and of the total test rig, providing an estimate of the mass loss rate of the linings. Total heat flux to different target points on the inner surfaces was measured using Schmidt-Boelter gauges and radiative flux was measured using Gunners type gauges. Gas temperatures within the enclosure(s) and in the openings to the outside were measured using trees of thermocouples of type K having a wire diameter of 0.5 mm, some of which were shielded from radiation. Pressure and oxygen

concentration were measured locally in a single position. Furthermore, the times to ignition of the linings and to flashover were evaluated using video recordings of the tests.
One conclusion from the single compartment tests was that the initial fire growth phase can be intimately coupled to the type of ignition source. This comes as no surprise since the heat flux from the flames and the hot gases is related to the, fuel dependent, soot fraction. The thermal characteristics within the enclosure at the time of flashover, however, proved to be largely unaffected by the initiation mode indicating flashover at a temperature in the gas layer of 650 °C and the thermal radiation to the floor of about 17 kW/m^2.

4. CFD modelling

Fire modelling using CFD techniques is a recognised field of research and of late it has become part of the everyday work in fire safety design, the most frequently modelled phenomena being the smoke movement in buildings. In comparing simulations with experimental results, several independent expert users have shown that the CFD codes having fire specific models implemented (such as CFX, FDS and SOFIE for example) do well in this regard. Caution is however required since there are indeed fairly simple scenarios in which the models seem to fail in their prediction, one such example being a single space with high ceiling[20,21].

An important insight is that a CFD solution does not claim to provide the correct answer to every scenario. We are still referred to the use of rather incomplete models in describing the course of events following a fire. The problems have been highlighted from a number of "blind simulations" in which a number of expert users simulate a scenario without prior knowledge of the end-results. Not surprisingly, the simulation results have been found to be both user and code dependent. Similar exercises have been performed within the fire modelling community covering zone models as well as various CFD software[22,23].

4.1 Computational Fluid Dynamics, CFD

The possibilities to obtain numerical values on important, fire related, parameters on a fine mesh of cells and to perform calculations which were beyond reach just a decade ago are appealing. Moreover, it is deceivingly easy to be seduced by the pretty pictures that are produced by the post processing software. Thus, for the credibility of CFD modelling as part of fire safety engineering it is essential that, for every new simulation, the users put careful attention to what, and to some extent how, the computer are actually calculating. A review of the theory behind CFD is not an issue of this report, several books and papers on the subject being readily available. Furthermore, the specific algorithms used in the CFD code FDS[27] have been addressed in numerous papers and reports and will not be fully reproduced here, some limiting models which are of importance in the flame-spread calculations are, however, presented and discussed below.

The basis of CFD are the conservation principles stating that mass, momentum and energy are conserved. Most of the computer programs dealing with turbulent reacting flows are based on a set of numerical techniques referred to as the finite volume method (FVM) using the integral form of the conservation equations as starting point.[24,25] The core equation of the FVM is exemplified, for a variable ϕ, in Eq. 2. From the left we have the time rate of change inside a volume denoted Ω, then transport due to convection through the surfaces enclosing the

volume and likewise, diffusion through the faces of the volume, the last term is a sourceterm referring to the destruction or production of ϕ within Ω).

$$\frac{\partial}{\partial t}\int_{\Omega}(\rho\phi)d\Omega + \int_{S}(\rho U)\phi\cdot \mathrm{n}dS = \int_{S}(\Gamma\nabla\phi)\cdot \mathrm{n}dS + \int_{\Omega} q_{\phi}d\Omega \qquad \text{Eq. 2}$$

In order to model the continuous phenomena of fluid flow the physical space is subdivided into a large number of finite volumes, called control volumes, on which equation 2 is discretised and solved using various finite difference approximations for the different terms. Algebraic interpolation is used to determine variables on the faces of the control volumes, a potential source of error. Due to the limitations in computer power, the discretisation cannot be made sufficiently fine to include all the relevant physics. Turbulence, combustion, radiation and boundary layer effects are all examples of phenomena that require some kind of simplification and modelling.

4.2 Some features of FDS

In the boundary layer near the walls the turbulent flow is influenced by viscosity and is slowed down due to wall friction. This induces steep gradients in terms of turbulent viscosity and velocity, since the instantaneous velocity components are zero at the solid boundaries (no-slip boundary). Temperature and enthalpy gradients are also generated due to the difference between the solid- and gas-phase temperatures. To capture these gradients in a numerical simulation, the transport equations would need to be integrated through the entire wall boundary layer. Very small control volumes are required for this task, so small that the cost in computational time is too great for all but the most trivial scenarios. A common solution is to use some kind of semi-empirical wall function to model the characteristics of the boundary layer, perhaps the most well-known being the the “law of the wall” approach[26].

In contrast, the CFD code FDS does not employ this concept but uses other empirical correlations for the wall flow[27]. Convective heat transfer to the wall, for example, is calculated using the largest value for the free and the forced convection respectively

$$\dot{q}''_{convective} = \Delta T * \max\left[C\left|\Delta T\right|^{1/3}, 0.037\frac{k\,\mathrm{Pr}^{1/3}}{L^{0.2}}\left(\frac{|\mathbf{u}|}{\nu}\right)^{0.8}\right] \qquad \text{Eq. 3}$$

Chemical kinetics has its own time and length scales, the phenomenon generally being much too complex and computationally expensive to be included, even in reduced form, in practical

CFD simulations[*]. Instead, in most fire modelling codes, combustion is calculated from the mixing rates of fuel and oxidant. Chemical reactions between fuel and oxygen are taken to follow a single, one-step stoichiometric reaction.

FDS uses a rather simple method based on oxygen consumption calorimetry for estimating the local rate of heat release. The oxygen consumption is calculated from the mixture fraction and the corresponding rate of heat release can then be evaluated from[27].

$$\dot{q}''' = \dot{m}_{O_2}''' \Delta H_{c,O_2} \qquad \text{Eq. 4}$$

In addition, a scheme is employed for relating flame extinction to the temperature and the oxygen concentration. In principle, this appears to be useful in simulating under-ventilated fires, where most CFD codes fail to predict burning behaviour accurately[†].

Another main challenge in fire modelling is heat transfer through thermal radiation which is of great importance in almost all fires of practical interest, representing the major contribution to the total heat flux. From a modelling standpoint, radiative heat transfer exerts its numerical influence through the energy conservation equation, where it appears as a source term that needs to be modelled. The radiation intensity varies with the wavelength, thus in principle requiring one equation for every wavelength. This would be too costly in terms of computational time and computer resources, the solution being to appriximate the radiation spectrum as being constructed of a number of bands, representing the spectral dependencies of the most important participating media, such as carbon dioxide and water. Using this assumption only one equation need to be solved for each spectral band. In most practical fire scenarios however, the radiative properties of the combustion products are governed by soot which has a rather continuous radiation spectrum. Thus, the gas volume can often be assumed to behave like a grey gas.

The radiation transfer equation ignoring scattering effects by soot, effectively assuming that all soot particles are small compared with the thermal radiation wavelength, is written

$$\frac{dI}{ds} = \kappa_a \left(I_b - I \right) \qquad \text{Eq. 5}$$

[*] In fact, the detailed reaction mechanisms are unknown in the case of most practical fuels. Yet even if all the details of these chain reactions were known, their implementation into a global model would be of little interest because of the computational cost.

[†] Although this method will not make FDS capable of actually handling under-ventilated fires, it is likely that also this crude model makes the code perform better than it would have otherwise.

While soot has a rather simple spectral dependency the local soot concentration in and near the flame is not generally known. Moreover, since radiation is proportional to the temperature raised to fourth power, a seemingly small error in the prediction of the gas temperature, which is quite likely in FDS (as well as most CFD codes used by the fire modelling community) due to the simple combustion model, can have an unacceptable influence on the end-result. Thus, in order to minimize these effects in FDS, blackbody intensity, I_b, takes its traditional value only outside the flame zone. Inside the flame the thermal radiation is simply assigned as a fraction of the local heat release rate[27]. This simplification is likely to have a fundamental influence on the radiation heat flux prediction.

$$\kappa_a I_b = \begin{cases} \kappa_a \sigma T^4 / \pi & \text{outside flame} \\ \chi_{loc} \dot{q}''' / 4\pi & \text{inside flame} \end{cases} \qquad \text{Eq. 6}$$

5. Pyrolysis modelling

Combining the CFD simulation of a turbulent reacting wall flow with a material model for transient heating and pyrolysis opens up possibilities for more flexible overall flame-spread models capable of dealing with the actual physics involved. The present trend represents a logical continuation starting with the work on the thermal modelling approaches that has been the most widely recognised engineering tool before.

5.1 General

The core of this report is a scenario involving flame spread and a following flashover in compartments where the major fuel source is a wooden based material. The chemical composition of wood is slightly different depending on what species are being studied. Generally speaking, however, wood can be said to be constructed from cellulose, hemi-cellulose and lignin where cellulose, with a chemical representation written as $(C_6H_{10}O_5)_n$, constitute about 50 % by mass. The process of the volatilisation of the different constituents is somewhat different resulting in different fraction of residual char, as shown in Figure 6.

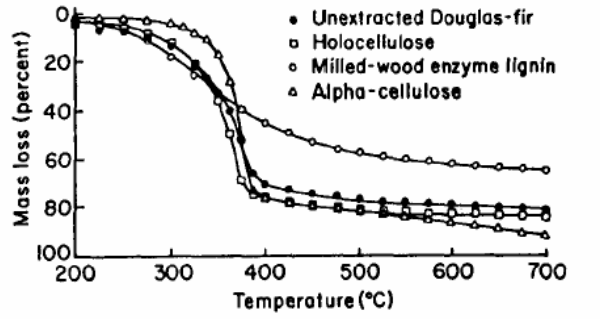

Figure 6. Mass loss of isolated wood components (Douglas fir) heated in nitrogen environment at 5 °C/min. From reference 28.

Furthermore, the timescales of degradation of the different constituents are depicted in Figure 7, where the difference is quite evident. Two conclusions can be drawn from the diagram. First, simplifying the pyrolysis kinetics to a one-step global reaction may be overly crude, three different pyrolysis reactions, one for each major component of the wood, possibly needing to be taken into account. Secondly, at high temperatures the thermal waves are rate-determining whereas at lower temperatures the kinetic time scale is comparable to the thermal time and may also be rate-determining.

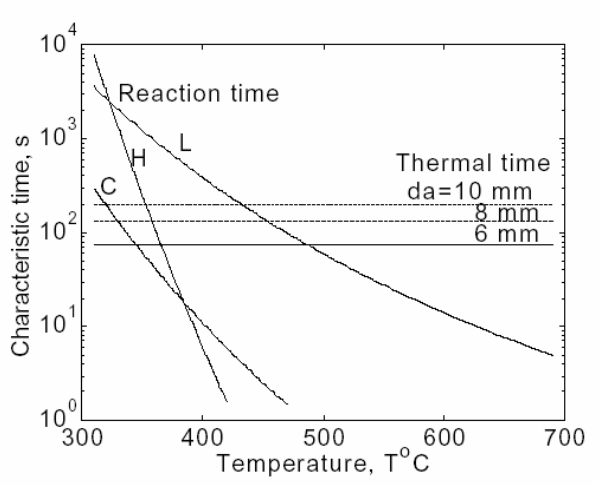

Figure 7. Illustration of the characteristic time scales of kinetic and thermal processes. C=Cellulose, H=Hemicellulose and L=Lignin. From reference 29.

It seems that the three major constituents needs separate treatment. This is problematic since the rate determining coefficients are very difficult to obtain and literature data scatter, sometimes with several orders of magnitude.

Another difficulty is how to treat the chemical reaction itself. A simple scheme can be written as below. Again, although a phenomenological description can be provided problems arise when it comes to practical engineering modelling. Lack of reliable input data and issues concerning computational cost put serious constraints on the flame spread modelling capabilities of current fire engineering tools.

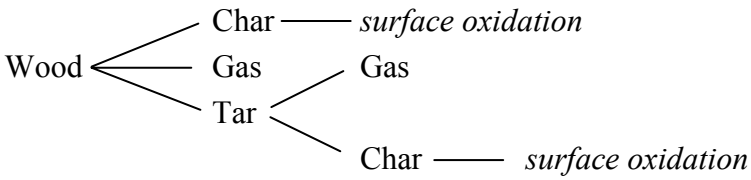

Figure 8. A simplified description of the pyrolytic process although perhaps too comprehensive to be used in practical engineering calculations of flame spread.

5.2 Pyrolysis modelling in FDS

The modelling tool used in this work is version 2 of the NIST CFD code FDS[27]. The flame spread modelling capabilities of FDS2 relies mostly on a model first proposed by Atreya[13]. It is based upon the assumption that there are no pressure gradients in the combustible material so that any mass transport within the material can be ignored, thus assuming water vapour and pyrolysis gases to reach the solid surface instantaneously. Applying this assumption the

complex process of pyrolysis is converted into a rather straight forward heat transfer problem. The overall equation can be expressed then as[12]

$$\overline{\rho c_p}\frac{\partial T}{\partial t}=\frac{\partial}{\partial x}\left(k_w\frac{\partial T}{\partial x}\right)+\frac{\partial \rho_w}{\partial x}\left[\Delta H_{py}-C_1\left(T-T_0\right)\right]+\frac{\partial \rho_m}{\partial x}\left[\Delta H_{ev}-C_2\left(T-T_0\right)\right] \qquad \text{Eq. 7}$$

to which standard boundary conditions are applied at the exposed surfaces and on the back surface of the combustibles.

In equation Eq. 7 the coefficients C_1 and C_2 represent calculated average values of the specific heat for the wooden material and for moisture respectively, ρ_w is the total density of the wood, and ρ_m is the density of the moisture, ΔH_{py} is the heat of pyrolysis treated as being a constant and ΔH_{ev} represents the heat of water evaporation. The overbar indicates that the parameters are evaluated at the average of the momentary temperature, T, and the initial temperature, T_0. At the evaporation temperature, all the energy available is used for evaporation of moisture but because of the constant pressure assumption, no moisture transport is seen as taking place inside the material. Both moisture and pyrolysis gases reaching the surface immediately since the momentum equations are not solved within the material.

The rate of pyrolysis is estimated using a single-step Arrhenius rate law of the first order, written as $\frac{\partial \rho_w}{\partial t}=-\rho_a A e^{-E_a/RT}$, where A is the pre-exponential factor, E_a is the activation energy and ρ_a is the remaining unburned fuel. These parameters are probably the most difficult to choose when using a model of this kind. In this study we rely on the use of trial and error calculations where parameters are adjusted to make the end-result agree with small scale experimental data.

In the version that followed FDS2, namely FDS3, the pyrolysis model does not seem to work very well (the problems could be traced back to the generation of the subgrid within the solid) and in the latest version, FDS4, the flame spread modelling capabilities have been simplified beyond recognition in order to make it easier to use in everyday simulation work[30]. Thus, FDS2, using the model equations introduced above has been used here.

6. Modelling heat transfer and ignition of combustible solids

The purpose of this chapter is to derive a set of input data that can be used by the pyrolysis model when performing the flame spread in simulations. This includes the development and use of tailor-made computer programs for calculating the heat transfer in 1D as well as 3D scenarios and comparing the model predictions with experimental data from the small scale tests, thus using a systematic trial and error approach to obtain parameter values corresponding to a best fit to surface temperature measurements, ignition data and the rate of heat release. The drawbacks in using the Cone Calorimeter for this purpose were discussed in section 3.2, what is important to keep in mind is that the apparatus was never intended as a modelling tool but as a means of classification, comparing the burning behaviour of different materials with each other. The major factor of uncertainty in the tests using a laser heat source is believed to be connected to scaling effects.

6.1 Deriving the thermal properties

The basic assumption in deriving the thermal properties of a sample material is that the change in surface temperature history reflects the heat transfer into the material such that given a correctly predicted surface temperature, the temperature distribution within the material can be expected to be adequately predicted as well. The procedure of obtaining the thermal properties of the sample material includes an iterative approach where the thermal conductivity and the specific heat are systematically optimised to obtain the best correlation to the experimental data. The predictions are compared to experimental data from the laser ignition tests, described in section 3.1, and from the cone calorimeter, see section 3.2. The final choice of input data obtained from such a procedure for medium density fibreboard, MDF, is given in Table 1.

Table 1. Input data obtained from successive surface temperature calculations and corresponding to a best fit to surface temperature measurements.

Property	**Assumed value**
Density (ρ)	780 kg/m^3
Emissivity (ε)	0.95
Specific heat (c_p)	(875.0 + 2.0·Temp (K)) W/m^{2}K
Thermal conductivity (k)	($3.15\cdot10^{-2}$ + $3.85\cdot10^{-4}$·Temp(K)) W/mK

In the Cone Calorimeter, the test sample is exposed to a uniform heat flux over its whole surface with its boundaries well insulated, therefore, in these tests, the heat flux can be assumed to be one dimensional thus greatly simplifying the heat transfer equation. In the laser induced ignition experiments on the other hand, the heat exposure was limited to a small part of the board effectively representing a three dimensional problem. Some of the results from the heat transfer simulations are presented below.

6.1.1 3D heat transfer in the laser induced ignition experiment

The general equation for heat conduction in a solid is reproduced in Eq. 8, the underlying physical meaning being that in the absence of heat generation within an element the heat is either conducted through the element or stored inside it giving raise to a change in temperature.

$$\nabla \cdot \left(k \nabla T\right) = \frac{\partial}{\partial t}\left(\rho c T\right) \qquad \text{Eq. 8}$$

In the experiments using a laser beam as heat source, the heat exposure was uniform with a circular shape. This is fortunate since it provides the opportunity to treat the scenario as an axisymmetric case, thus simplifying the computational task considerably.

As an initial condition the temperature is normally assumed to be evenly distributed at some initial temperature, $T(x,0) = T_0$. The boundary condition at the front surface of the solid is written as

$$\dot{q}''\left(0,t\right) = -k\left.\frac{dT}{dx}\right|_{x=0} = \alpha \dot{q}_e'' - h_{conv}\left(T - T_0\right) - \varepsilon\sigma\left(T^4 - T_0^4\right) \approx \dot{q}_e'' - h\left(T - T_0\right) \qquad \text{Eq. 9}$$

Where, in the last step, the absorptivity α is assigned a value of unity and the heat losses are bracketed into a single, yet highly non-linear relationship, h. It is noted that although such an expression is handy when approximating the heat transfer rate using a hand calculation methodology it has no merit when solving the equations numerically. The temperature dependence on the convective heat transfer coefficient, h_{conv}, can be taken account for through the Grashofs number, basically relating the buoyancy force to the viscous drag in the boundary layer. The end result for the calculations performed here however, being only slightly affected by this dependency.

Regarding the test sample as being thermally thick gives the following boundary condition for its rear surface:

$$T(\infty, t) = T_0 \qquad \text{Eq. 10}$$

The above equations were solved using the axisymmetric assumption to obtain the surface temperature as function of time. Figure 9 illustrates how the surface temperature of the sample changes at the edge of the exposed area when the external heat flux is 20 kW/m^2. Comparisons of surface temperature between experimental data, as measured using a thermocouple, at this same heat flux as well as for 40, 60 and 80 kW/m^2 are presented in Figure 10.

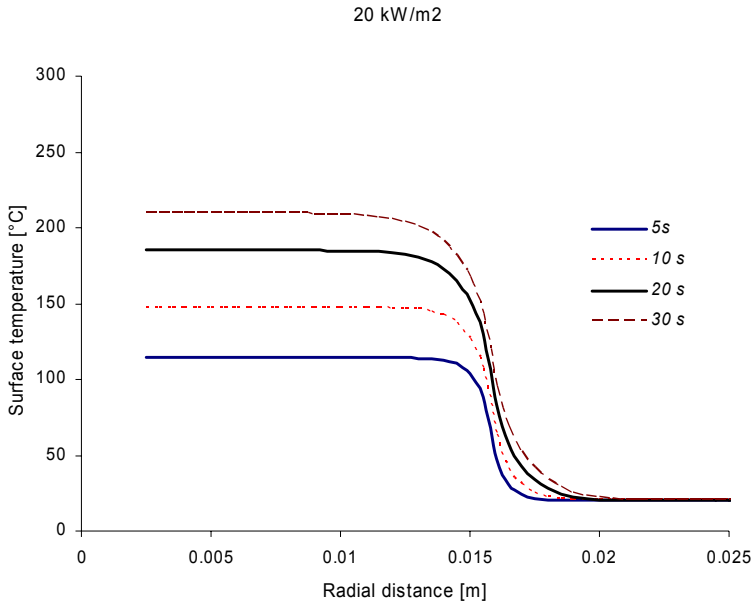

Figure 9. Surface temperature distribution over the face of the sample.

The agreement between the computed temperatures and the thermocouple measurements are, on the whole, within the measuring error. For the lowest heat flux, at 20 kW/m^2, the results are excellent, the divergence for the early temperature rise however, amplifies gradually as the external heat source is increased. Possible explanations to this behaviour are likely to be found from the thermocouple measurements but can also reflect a deficiency in the external heat source as well as simplifications made in the modelling strategy. Searching physical explanations in material response to different levels of heat flux becomes even more speculative.

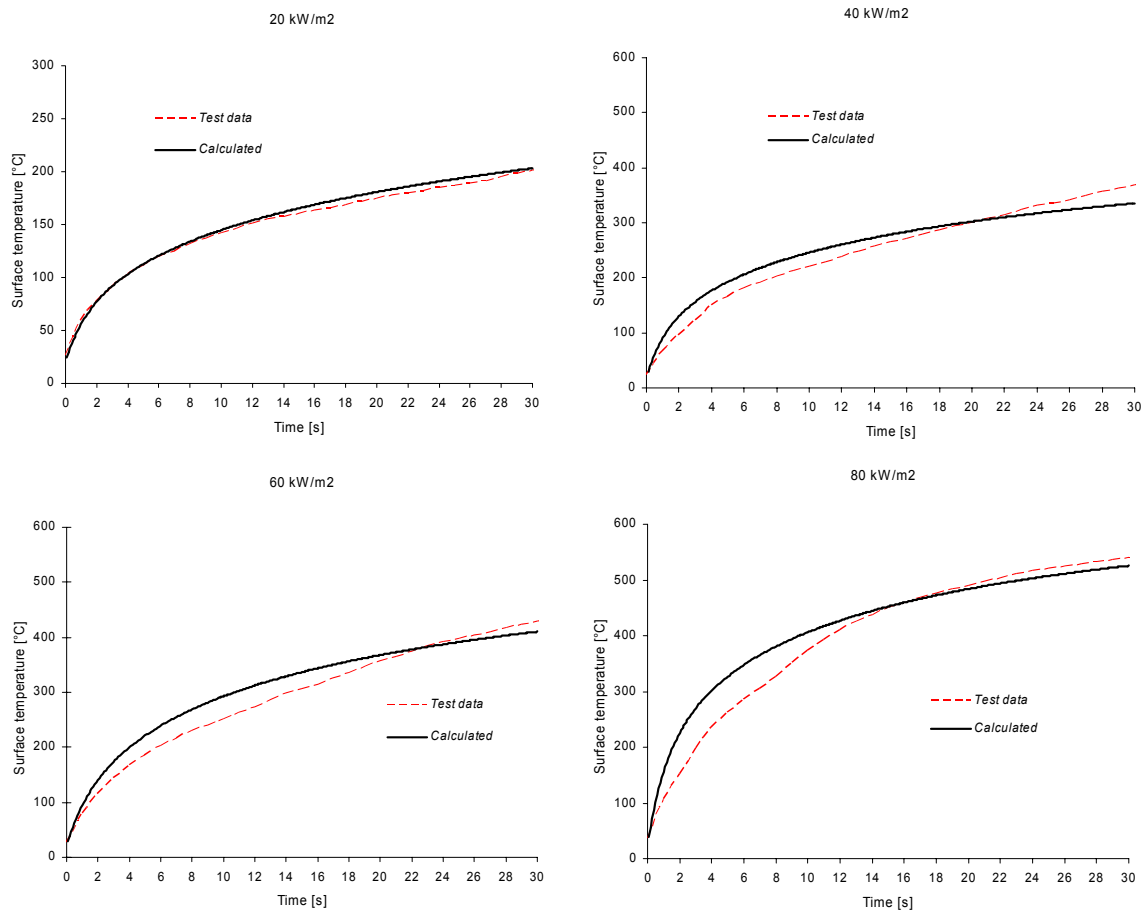

Figure 10. Calculated average surface temperature over the exposed area compared with thermocouple measurements.

6.1.2 One dimensional heat transfer in the Cone Calorimeter

The cone calorimeter is constructed to promote one dimensional heat transfer through the test sample. For this case the general heat conduction equation is simplified to

$$\frac{d}{dx}\left(k\frac{dT}{dx}\right)=\frac{d}{dt}\left(\rho cT\right) \qquad \text{Eq. 11}$$

It may be that a test sample in the cone calorimeter is subjected to some degree of preheating before the cone has reached the required heat flux. This is however, rather difficult to take into account due to the lack of data, thus the initial and boundary conditions from the last section still holds and the numerical solution is straightforward. Figure 11 presents a comparative analysis at a heat flux of 15 kW/m^2. The thermocouple data is extracted as an average value, the different thermocouple measurements, however, start to deviate somewhat after about three minutes of exposure.

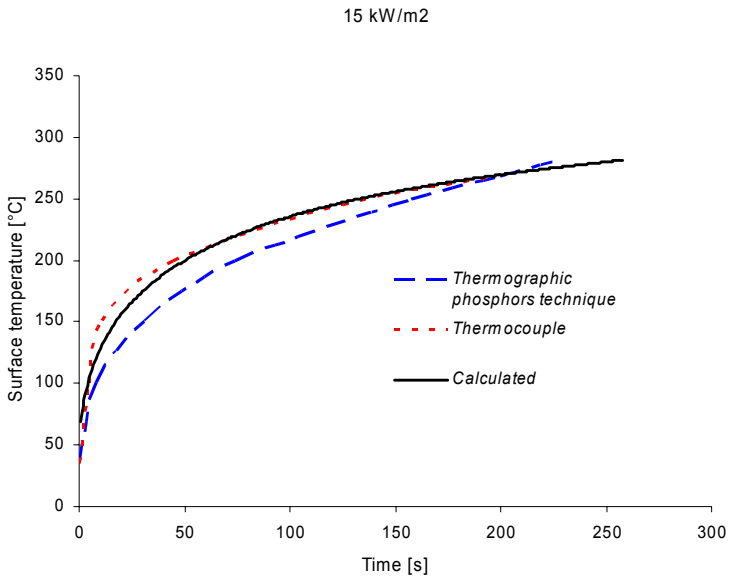

Figure 11. Calculated surface temperature using the heat conduction, Eq. 11, compared to measurements using thermocouples and a thermographic phosphors technique. Experimental data from reference 31.

The above calculation uses the same input data as in the axisymmetric analysis in the previous section. The agreement between the thermocouple data and the computed surface temperature is very good. The readings obtained using the thermographic phosphors technique however, deviate slightly suggesting a lower surface temperature then the other two graphs. Göransson and Omrane[31] argue that both these measurement techniques should be expected to give the wrong answer since strictly neither measure the actual surface temperature.

6.2 Deriving the pyrolysis parameters

The pyrolysis models presently available to the fire safety community all include rather crude assumptions. The model implemented into FDS2, as described in section 5.2 being no exception. However, using Arrhenius based kinetics to predict the decomposition as function of temperature and remaining fuel (if "only" a first order, single step function) this is one of the most complete models currently available as part of a fire dynamics CFD code.

Despite (or perhaps due to) the simplifications, input data to any pyrolysis- and fire growth model are very difficult to find from the literature. Reported data for the activation energy and the preexponential factor can differ by several orders of magnitude for the very same material. Thus, similar to the derivation of the thermal properties, obtaining adequate decomposition parameters generally include an iterative or a "trial and error" procedure where different combinations of input data are compared with available experimental findings on parameters such as time to ignition, rate of heat release and mass loss rate. Although it is recognised that

the outcome from the Cone Calorimeter was never intended for direct quantitative use, this is basically the only source from which enough of data are available at this time.

Using the thermal properties as previously derived, only the heat of pyrolysis and the Arrhenius parameters, E_a and A_p, need to be addressed in this analysis. A reasonable agreement was found using the parameter values given in Table 2, in which the thermal data are also reproduced for clarity. It is further recognised that both the activation energy and the pre-exponential factor differ somewhat from literature data.

Table 2. Summary of input data derived from test data on surface temperature, heat transfer and pyrolysis.

Property	**Assumed value**
Density (ρ)	780 kg/m^3
Char fraction	0.10
Emissivity (ε)	0.95
Specific heat (c_p)	(875.0 + 2.0·Temp (K)) W/m^{2}K
Thermal conductivity (k)	($3.15\cdot10^{-2}$ + $3.85\cdot10^{-4}$·Temp(K)) W/mK
Preexponential factor (A_p)	$1.19\cdot10^{2}$ s^{-1}
Activation energy (E_a)	$5.4\cdot10^{4}$ J/mole
Heat of pyrolysis (H_{py})	$100\cdot10^{3}$ J/kg
Heat of combustion (ΔH_c)	$14.06\cdot10^{6}$ J/kg
Assumed flame heat flux	min(0.15·RHR,25) kW/m^2

Figure 12 shows a comparison between calculated and measured mass loss rate per unit area at a cone heat flux of 50 kW/m^2. In the early stages from ignition to about 5 minutes into the test the results are rather consistent. In the later stages however, the result depends heavily on the thickness of the sample as well as the boundary condition on the rear side of the test sample. Therefore, in order to partially avoid these characteristics, Figure 12 shows a simulation using a sample thickness of 25 mm.

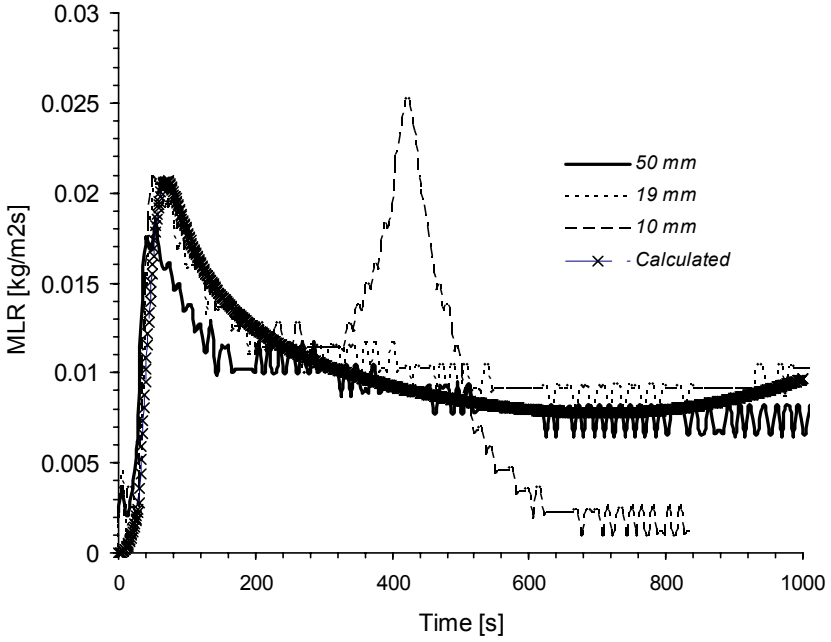

Figure 12. Comparison of calculated mass loss rate using input data from Table 2 with experimental data from reference 19 at an external heat flux of 50 kW/m^2. The computation refers to a sample thickness of 25 mm.

7. Flame spread simulations

The combination of a general CFD calculation of a turbulent reacting fluid flow with a model relating the heat flux to a combustible surface to the thermal decomposition of the material makes a basis for a potentially powerful flame spread model. In this chapter the CFD code FDS2 is evaluated in a study of flame spread and fire growth in three different geometries as described in section 3.3.

7.1 Single compartment scenario

The physical scale of this scenario is often referred to as a one third scale model. The basic configuration is a single fire compartment (0.8×0.8×1.1 m^3, width×height×depth) with one opening (0.3×0.6 m^2, width×height) and an initial fire source in the corner of the rear wall, opposite from the opening. Similar scenarios having an aspect ratio of 1-2 have been simulated previously in different "validation" exercises[4,10,11,12]. Moreover, Karlsson[7] demonstrated that a model based on rather crude assumptions on flame morphology, heat flux and thermal properties can be used to predict the flame spread and fire growth in a well defined one room configuration.

Only two out of five of the experiments performed in the one-compartment tests, presented in reference 3, have been analysed within the scope of this work. The restriction was made in order to reduce the number of simulations, thus allowing for a more in-depth analysis of the chosen scenarios, but also in view of the limitations stated by the models, perhaps the most important being that only one combustion reaction can take place during a simulation with FDS2. Thus, the simulations concern only the scenarios using heptane and wood as initial fuel source.

Figure 13 shows an example of the measured rate of heat release history, using heptane as initial fire, as evaluated from the gas analysis in the hood outside the room and from the mass loss measurement respectively. The O_2 calorimetry based data has been corrected for the time delay in the measurement. Clearly the two approaches provide similar results. In the following comparisons only one of these measurements will be reproduced, primarily the one based on the fire gas analysis. Figure 13 further include a simple approximation of ventilation control limit of the fire based on opening area (A) and opening height (h), this will be covered in some more detail later in this chapter.

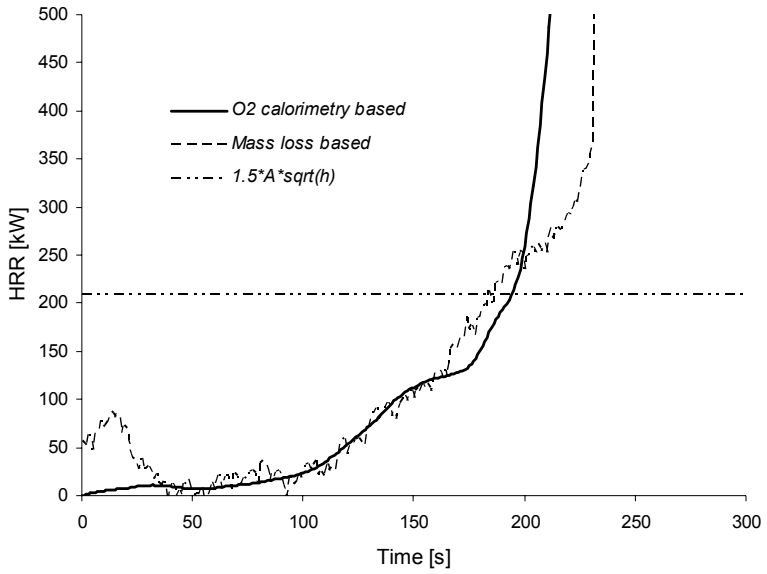

Figure 13. Total rate of heat release evaluated using gas analysis of the combustion gases and the mass loss rate through the expression $dQ/dt=\Delta H_c \cdot dm/dt$, respectively.

Certainly, simulations such as these are sensitive to the correct description of the initial fire source. The CFD code require information on the initial fire conditions prior to the fire spread in the compartment and although it may be possible to use the code itself in order to calculate the subsequent spread of flame and fire growth on the initial fuel surfaces such calculations are not recommendable at this time. Additionally, a limitation set by the FDS software is that only one fuel-air reaction can take place during a simulation. This means that the modeller needs to choose fuel according to the expected outcome of the simulation. For example, in the cases considered in the present report the MDF boards are considered to contribute the most to the fire heat release. The practical implication of this is that a scenario involving fuels having fundamentally different properties cannot be successfully analysed. Accordingly, the tests using methanol as initial fire could not be successfully dealt with here due to its low soot fraction, instead focus were put on heptane and wood cribs. The soot fraction of heptane is about 0.024 whereas wood (and fibreboard) can be assumed to have a soot fraction of about 0.015. Moreover, the net heat of combustion of wood is about 14 MJ/kg while the corresponding value for heptane being closer to 44 MJ/kg. These differences need to be kept in mind when evaluating the computational results.

In this work, two different approaches were used in describing the initial fire source to the CFD code. First, a constant rate of heat release was chosen, in the graphs to come this is emphasised using the identifier "Q_0=constant". This constant value was chosen based on an average heat release as obtained from the measurements, about 20 kW for the heptane fuel source, a short linear fire growth was assumed based ramping the HRR to its constant value in 20 seconds. Secondly, the mass loss of the initial fuel source given as input to the model was

chosen to coincide with the load cell measurements of the fuel trays containing the initial fires during the experiments. The approximations are illustrated in Figure 14. Using these curve-fitted initial fires, the actual heat feedback to the fuel surface is implicit in the input to the model. In the graphs that follows, simulations using this approach are tagged using the identifier "Q_0=variable".

Obviously, as can be seen from Figure 14 (b), the wood-crib fire source could not easily be approximated using a constant fire size in the same way as for the heptane fire. Therefore, only the approximation shown in the figure was used in these simulations

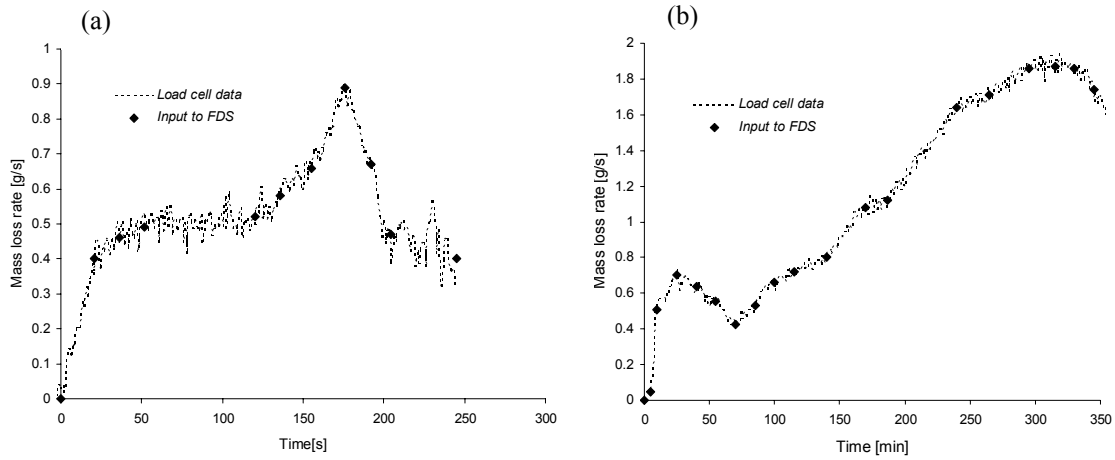

Figure 14. Mass loss rate of the initial fire source, heptane (a) and wood cribs (b). Note that in order to obtain the RHR given to FDS the heptane graph should be multiplied by the heat of combustion for heptane while the value of wood should be used when considering the wooden cribs.

Heptane fire source

The meshing initially used was of a cubical form, $\Delta x=\Delta y=\Delta z=0.02$ meters, which is about 1/10 of the characteristic fire diameter as defined by Eq. 12 and using a rate of heat release of 20 kW.

$$D^* = \left(\frac{\dot{Q}}{\rho_0 T_0 c_p \sqrt{g}} \right)^{2/5} \qquad \text{Eq. 12}$$

Figure 15 shows a comparison of measured and computed rate of heat release including several different simulations. The scenario relates to tests C2 and C4 in reference 3, one room lined with MDF board on its inner walls and under the ceiling and using a tray of heptane as initial fire source. From the calculated data it is clear that the simulations using a variable heat release rate or the initial fire according to Figure 14 is slightly higher during the first 2.5 minutes also going to flashover earlier than the simulation using a constant heat release or the initial source. The trend is however, similar for both these simulations.

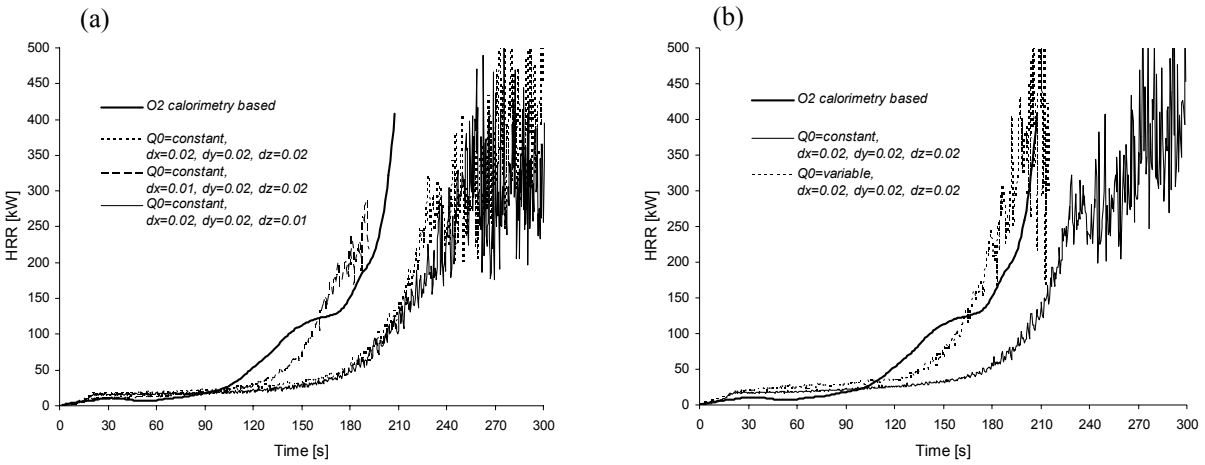

Figure 15. Total heat release rate using a heptane fire source to initiate flame spread and fire growth on MDF linings, comparison of measurement with calculations. The left hand figure (a) shows the influence of altering the grid size while the right hand figure (b) compare different strategies in describing the initial fire source.

Furthermore, Figure 15 illustrates the grid dependence of the simulations, taking as reference the scenario with cubical control volumes, 0.02 meters in side. From the results shown in this figure, it is evident that node independence cannot be claimed in this case. This is further emphasized in Figure 16 in which three simulations are compared, all three having a grid of cubical shape but with different side lenghts, that is 0.01, 0.02 and 0.03 meters respectively. The largest grid, although showing an initial growing trend, does not reach a state of flashover thus representing a fundamentally wrong solution to the scenario.

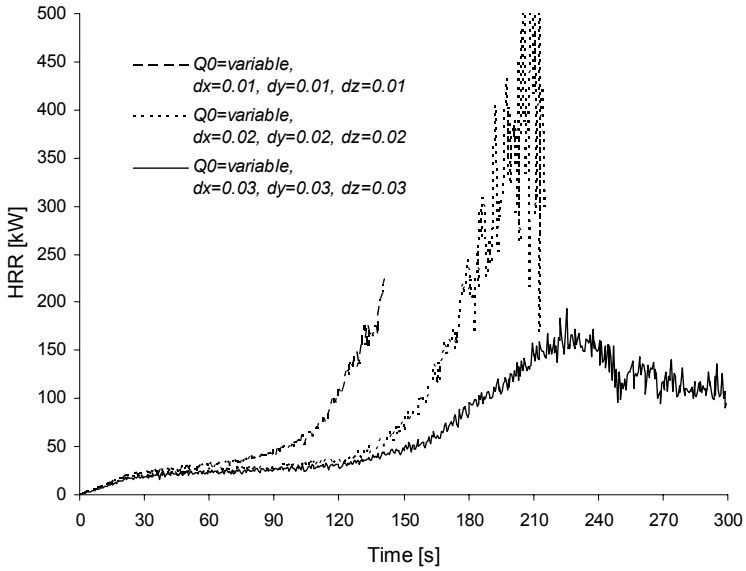

Figure 16. Diagram showing the node dependence in the one-compartment scenario using a heptane tray as initial fire source. The simulations are preformed assuming a variable heat release rate as adopted from load scale data.

It has been shown that the computation using the variable initial fire and cubical like control volumes with the side 0.02 meter provides good agreement with experimental data on the fire growth rate and time to flashover. While it may appear unsatisfactory that a node independent solution cannot be identified, it is still interesting to study this calculation more in-depth and compare the predictions on gas temperature and velocity with the experimental data.

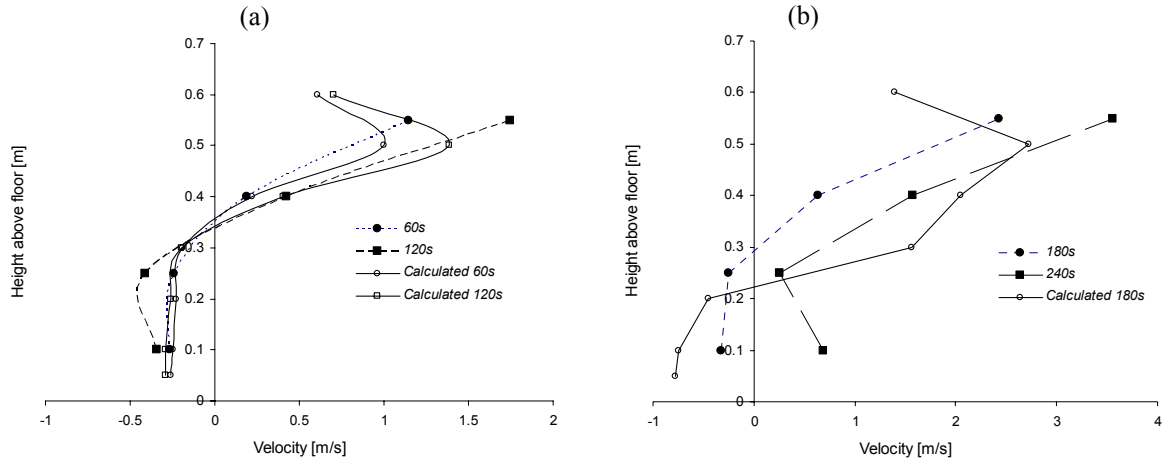

Figure 17. Comparison of experimental and predicted gas velocities in the compartment opening at different points in time plotted as function of opening height. Q_0=variable, dx=dy=dz=0.02 meters.

Comparing the computed results with the experimental data as presented in Figure 17 and Figure 18 reveal a similar trend to the one seen in the HRR prediction. The predictions are close to the experimental data but are somewhat dislocated in time in the later part of the scenario. This is further elucidated in Figure 19 in which the velocity and temperature of the gases exiting the compartment from the upper part of the door opening is displayed. It is also recognised that the experimental data in Figure 17 (b) indicates that the mass balance is not satisfied, this can be attributed to the transition from well-ventilated burning to flashover and ventilated-controlled burning.

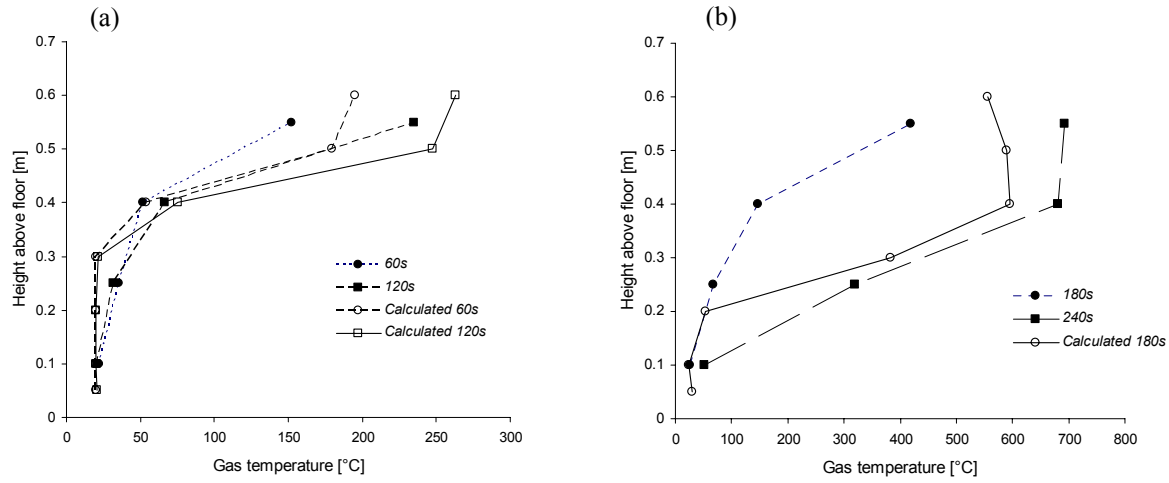

Figure 18. Gas temperature profiles in the centre of the door opening.

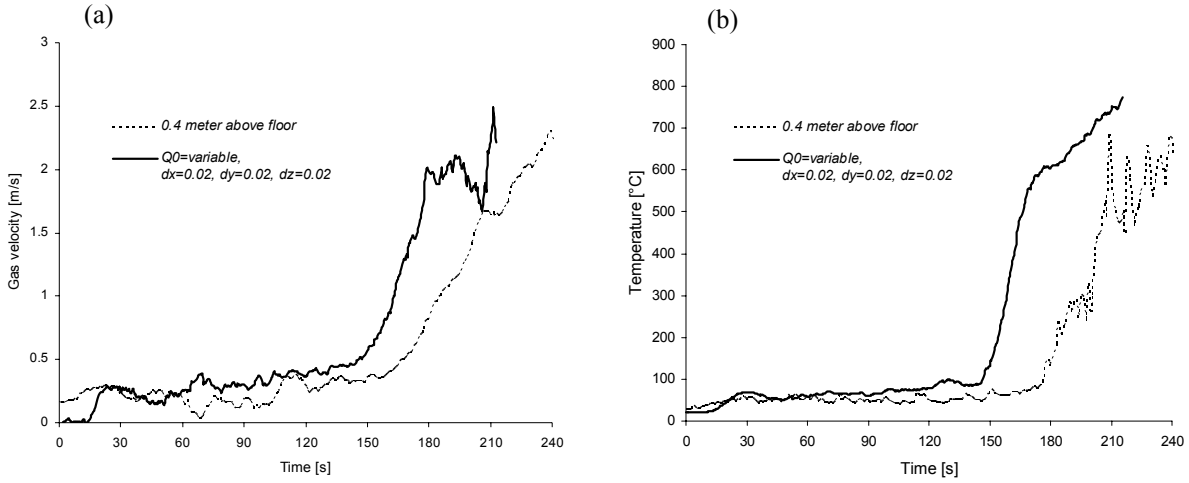

Figure 19. Computed and measured gas velocity (a) and temperature (b) results in the centre of the opening at 0.4 meters above floor.

Wood cribs

The second scenario of the one-compartment tests to be considered here is the one involving wooden cribs as initial fire source. In this case the properties of the initial source and the combustible linings are very closely related. This is likely one important explanation to the perfect agreement between the heat release rate obtained from gas concentration measurements in the duct and the one calculated from the mass loss rate data, see Figure 20. The ventilation conditions are the same as in the previous scenario, namely a single opening 0.3×0.6 meters between the fire compartment and its surroundings.

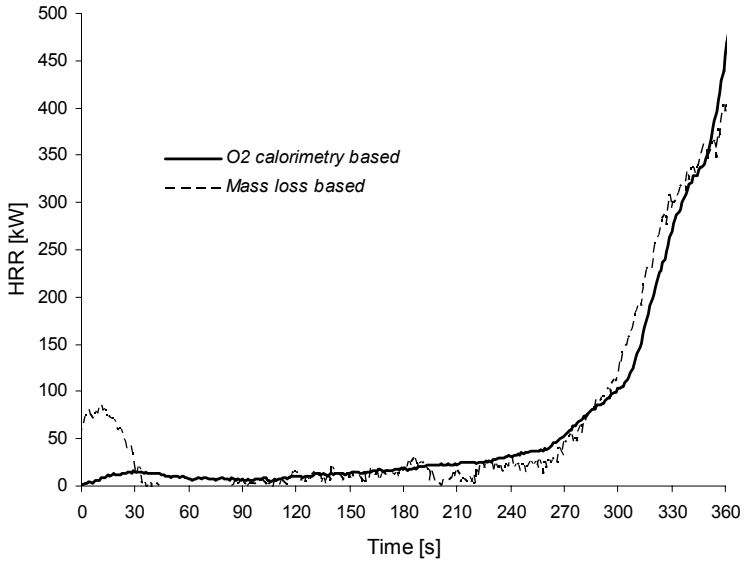

Figure 20. The total rate of heat release from tests using wooden cribs as initial source as evaluated with different techniques.

Similar to the results from the simulations using heptane as initial fuel, presented in Figure 15, the computational results from the scenarios with a wooden based initial fire suggest that a node independent solution cannot be found, the grid dependence is exemplified in Figure 21. The calculated result seems to be quite sensitive to grid changes in the x-direction (longside) whereas a change in grid size in the other directions (in Figure 21 exemplified using the vertical, z-direction) is less sensitive. The reason for this is likely to be found in the way the flame spread under the (combustible) ceiling. Nevertheless, the simulation using a cubical grid with side 0.02 meters and an initial fire adopted from the mass loss rate measurement of the wooden cribs once again provide good agreement with the experimental data.

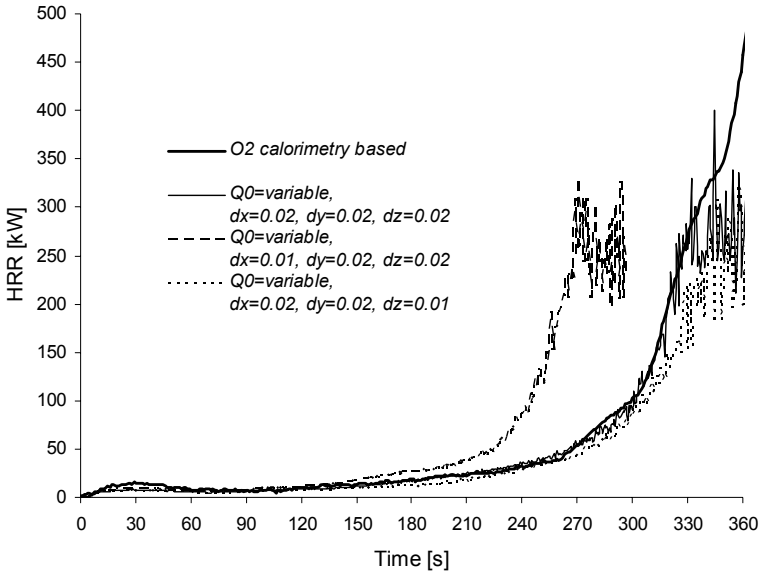

Figure 21. Measured and calculated rate of heat release using different computational grids.

In Figure 22, gas velocity predictions at a few selected points in time are compared with experimental data. The computation provides a reasonable match when compared with the experiment results. The gas layer interface is somewhat underestimated during the growth phase and the inflow patterns diverge from the test data.

Figure 23 further consolidate the solution as being physically correct considering the major parameters in the fire scenario. Figure 23 (d) suggests the simulation to be dislocated in time with about 15-20 seconds, somewhat overpredicting the time to flashover.

Similar to the previous scenario, the experimental result does not satisfy the mass balance in the later stages of the test, the most probable explanation being transient effects from the under-ventilated fire.

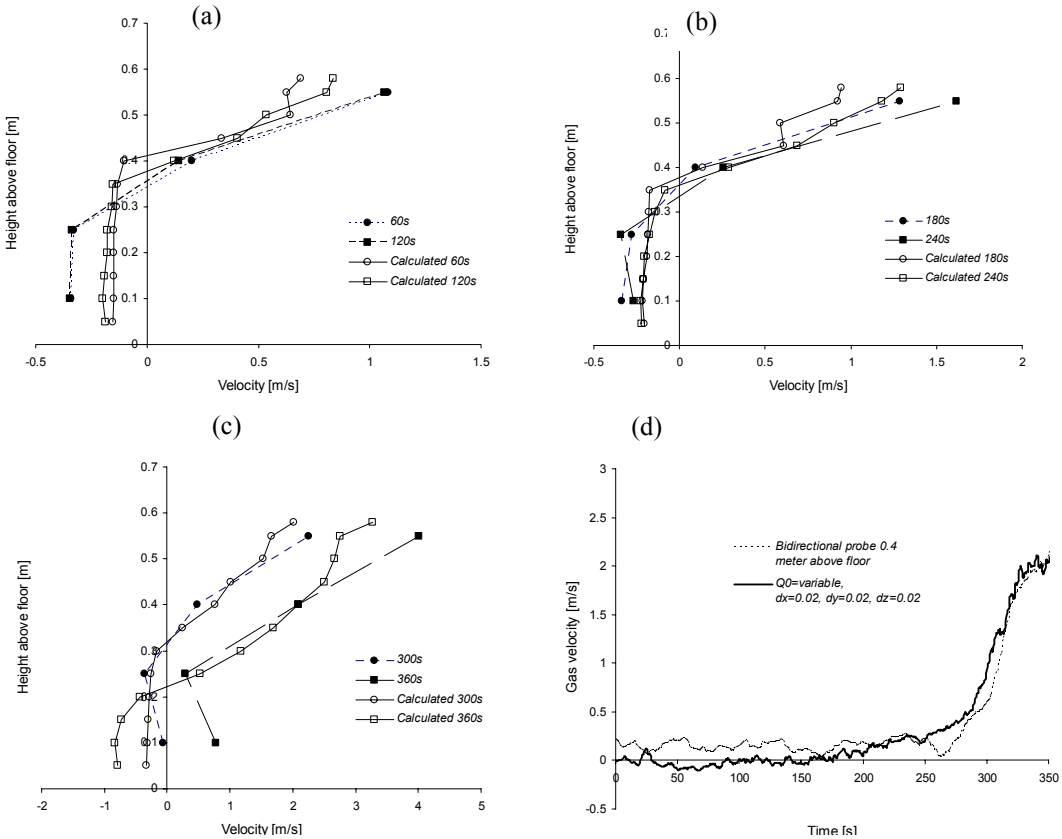

Figure 22. Computed and measured gas velocity in the vertical centreline of the door opening.

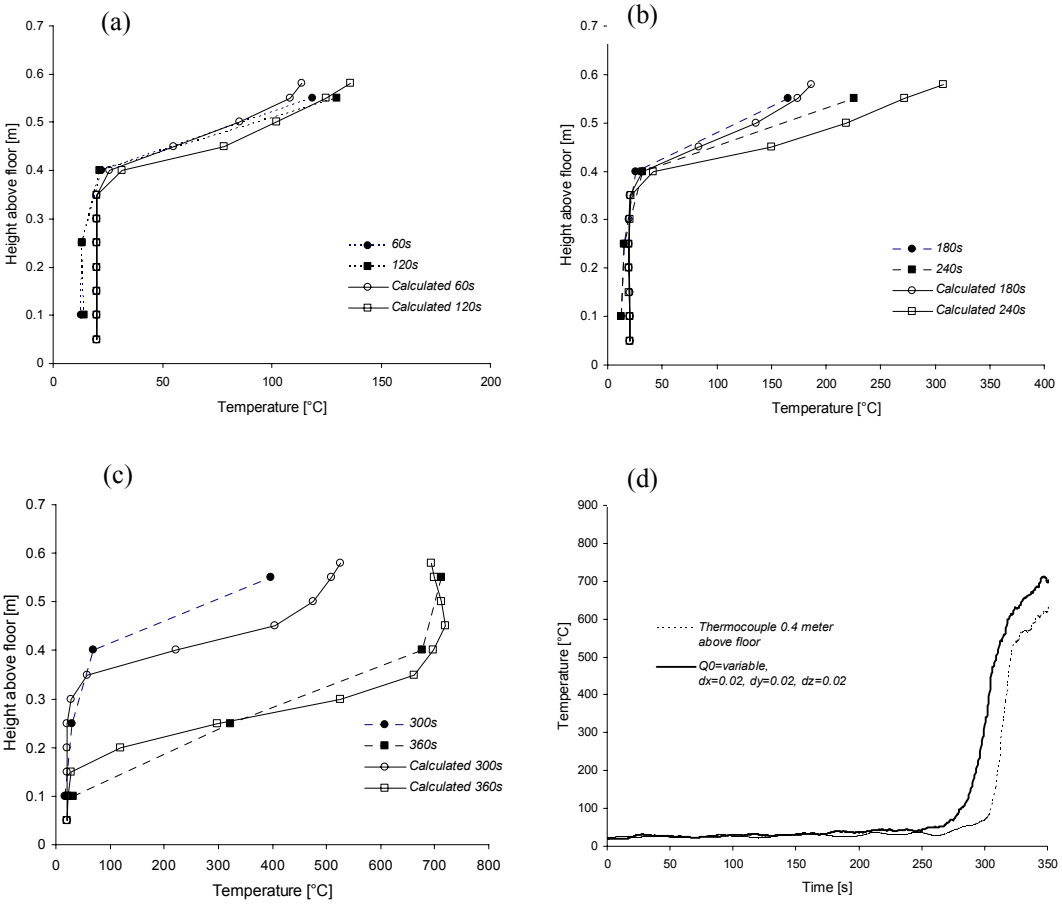

Figure 23. Comparison between computed and measured temperatures in the vertical centreline of the opening

The radiative heat flux to the floor was measured in a point on the centreline, at a 0.38 meter distance from the door opening. The results are shown, and compared with the computational result, in Figure 24. As could be expected, since the RHR prediction was indeed very good, the heat flux shows a great agreement with the experimental data. However, as is indicated in the diagram, the prediction falls apart after flashover showing a rapid decrease while the experimental result suggests a continuously high level of radiation to the floor.

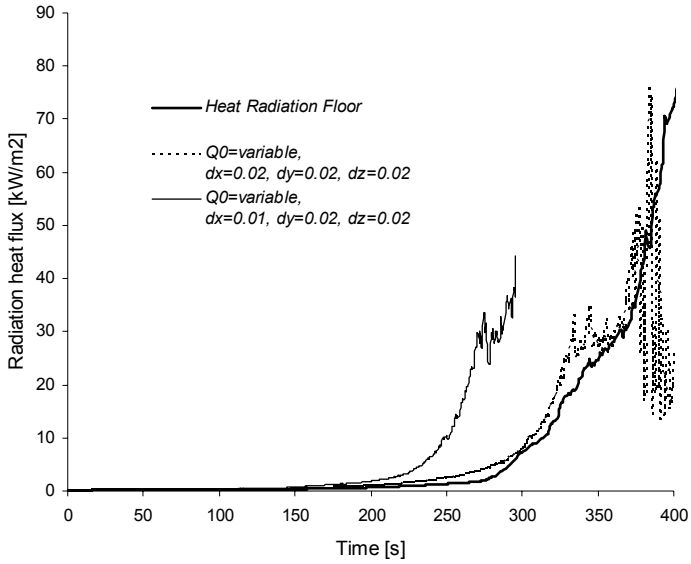

Figure 24. Predicted and measured radiation heat flux to floor, target is located on the centreline, 0.38 meters from the opening.

7.2 Two compartments in a vertical array

This section presents the results from experiments and simulations in which two compartments have been placed on top of each other, the compartments being connected through a horizontal opening. The initial fuel used in the experiments was heptane but again, due to the limitations of the CFD program, a fuel having wooden like characteristics, had to be used in the simulations. The size of the initial fire is approximated using either a constant or a curve-fit variation according to the mass loss measurements of the fuel tray.

The most interesting question to be answered in this and the following section (evaluating the results from two compartments linked in a horizontal array) is if the trends from the simulations of the single compartment can be reproduced, most interestingly if the simulation conditions offering good agreement with the experimental data in the single compartment tests do so also when the geometry has been changed, adding one compartment in the vertical or the horizontal direction. It should be emphasised that failing to do so will not automatically suggest the CFD code to produce inconsequent results on the incident heat flux, since it must

be bared in mind that the pyrolysis model as well as the input data to this model was derived assuming piloted ignition, the course of auto ignition being quite a different problem. The flame-spread between the two compartments may in fact be somewhere in between these two modes of ignition.

The analysis presented below includes only two from a total of five different experimental configurations described in reference 3. The selected scenarios are those referred to as V4 and V5 in reference 3, the ventilation conditions are reproduced in Table 3.

Table 3. Ventilation conditions for the scenarios considered in this section.

Vent condition	**V4 (W×H)**	**V5 (W×H)**
Door opening; fire room to outside	0.3×0.6	0.3×0.6
Door opening; top compartment	0.3×0.6	-
Opening between compartments	0.3×0.3	0.3×0.3

In evaluating the experimental data on fire growth, Figure 25, it is noted that the different measurement techniques does not correlate perfectly in time as was seen for the single compartment tests. This is likely caused by the accumulation of the combustion gases in the upper compartment effectively adding to the travel time of the combustion gases from the combustion zone to the position at which the gas analysis is carried out. The trend is nonetheless identical making easy to assume that the mass loss based result does represent a credible outcome of the fire growth rate in both scenario V4 and V5 also from a temporal point of view.

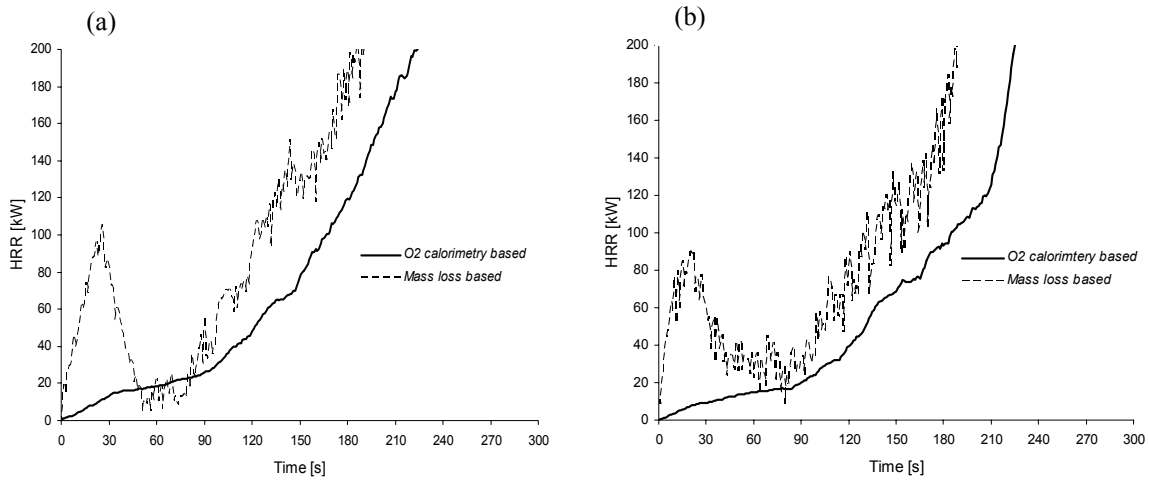

Figure 25. Total heat release rate for test V4 (a) and V5 (b) according to different measurement techniques.

Figure 26 shows a comparison between the measured data on the fire growth and computed results using cubical cells with the side length 0.02 meter. The simulation following the curve-fitted initial fire, derived according to the mass loss measurement of the fuel tray provides reasonable agreement with the experimental data, the onset of flashover being delayed by some 30 seconds compared with the load cell data. The simulation, in which the heat release rate is ramped from 0 to 20 kW in 20 seconds then held constant, shows an under-prediction of the time to flashover between half a minute to one minute as compared with the other simulation although it does give an identical fire growth rate. The seemingly small difference in the initial fuel source does indeed show significance in the later course of events.

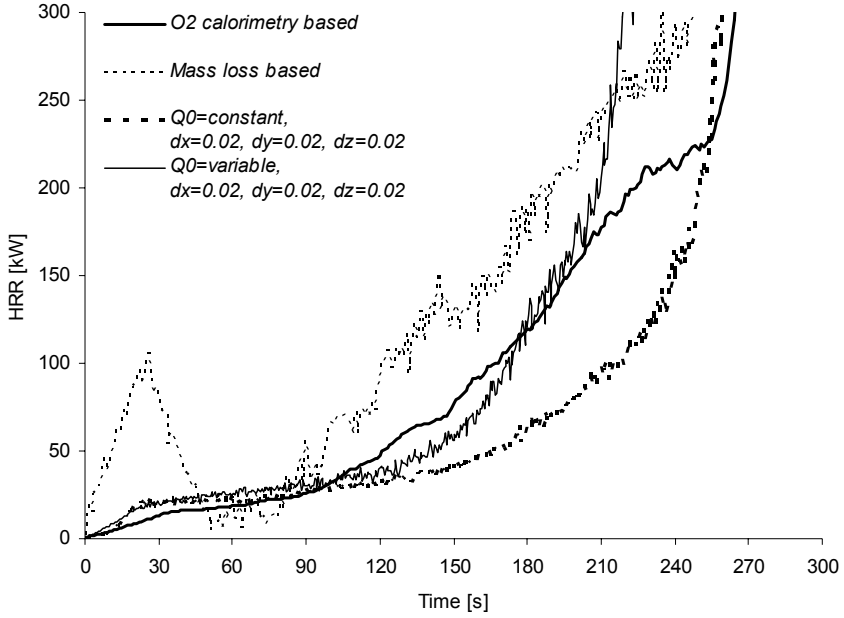

Figure 26. Total rate of heat release illustrating the fire growth on the compartment walls, comparison of measurement data and calculated results for test V4.

In Figure 27 the measured gas temperature in the fire room is compared with results extracted from the simulations. The result found here is direct corroboration of the results from the RHR comparison above, the data showing good agreement the first 3-4 minutes then overpredicting the rate of fire growth. A similar chart of diagrams, showing gas temperature predictions in the upper compartment is presented in Figure 28.

It can be concluded that the simulation predicts the gas temperature to a high level of accuracy as compared with the experimental data, noticeable especially in the upper compartment. This is however, somewhat clouded by the disagreement in mass balance over opening in the upper compartment, shown in Figure 29.

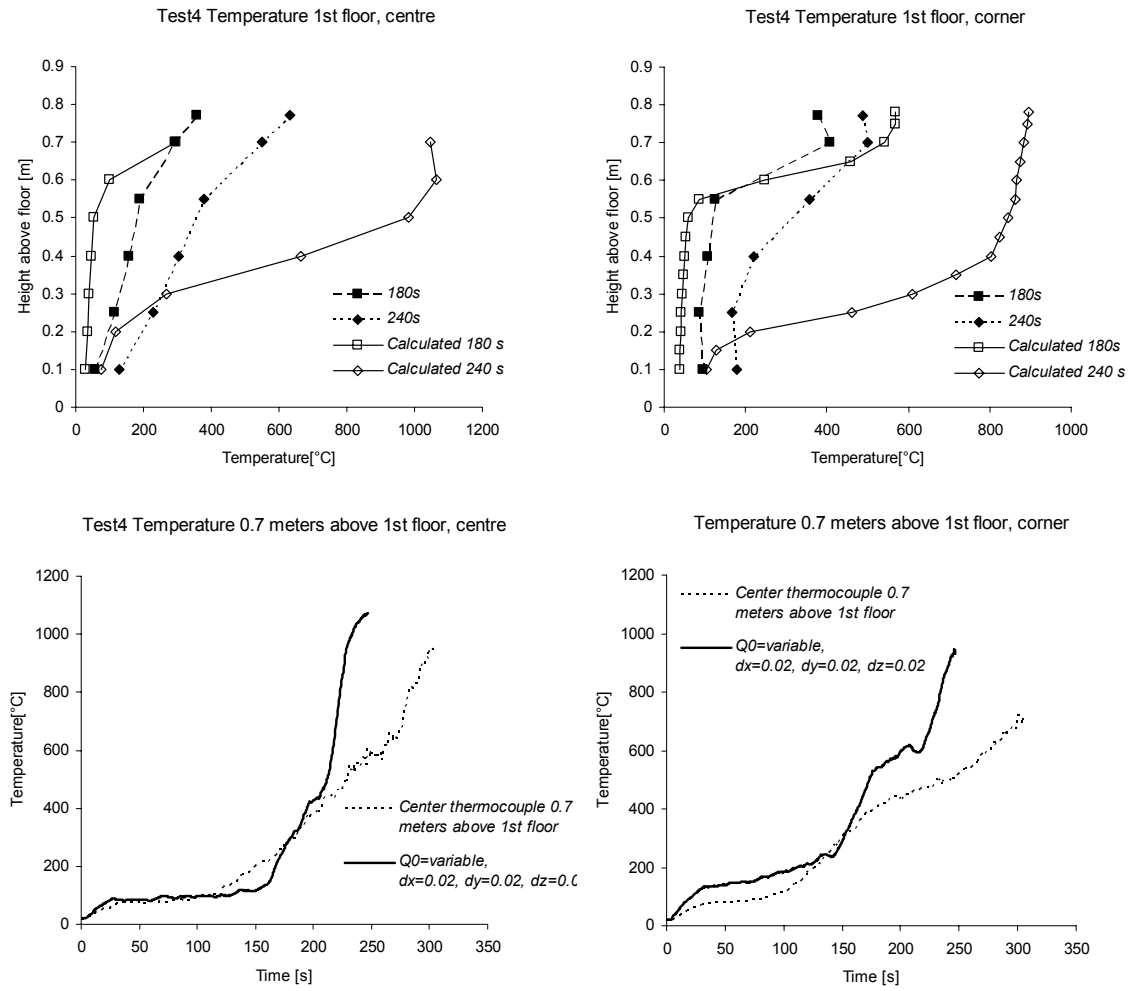

Figure 27. Comparison between predicted and measured gas temperature at some selected points in time and space in the fire compartment. All the predictions refer to the simulation using a curve-fitted initial fire and with the computational domain meshed according to a cubical form control volumes with 0.02 meter side.

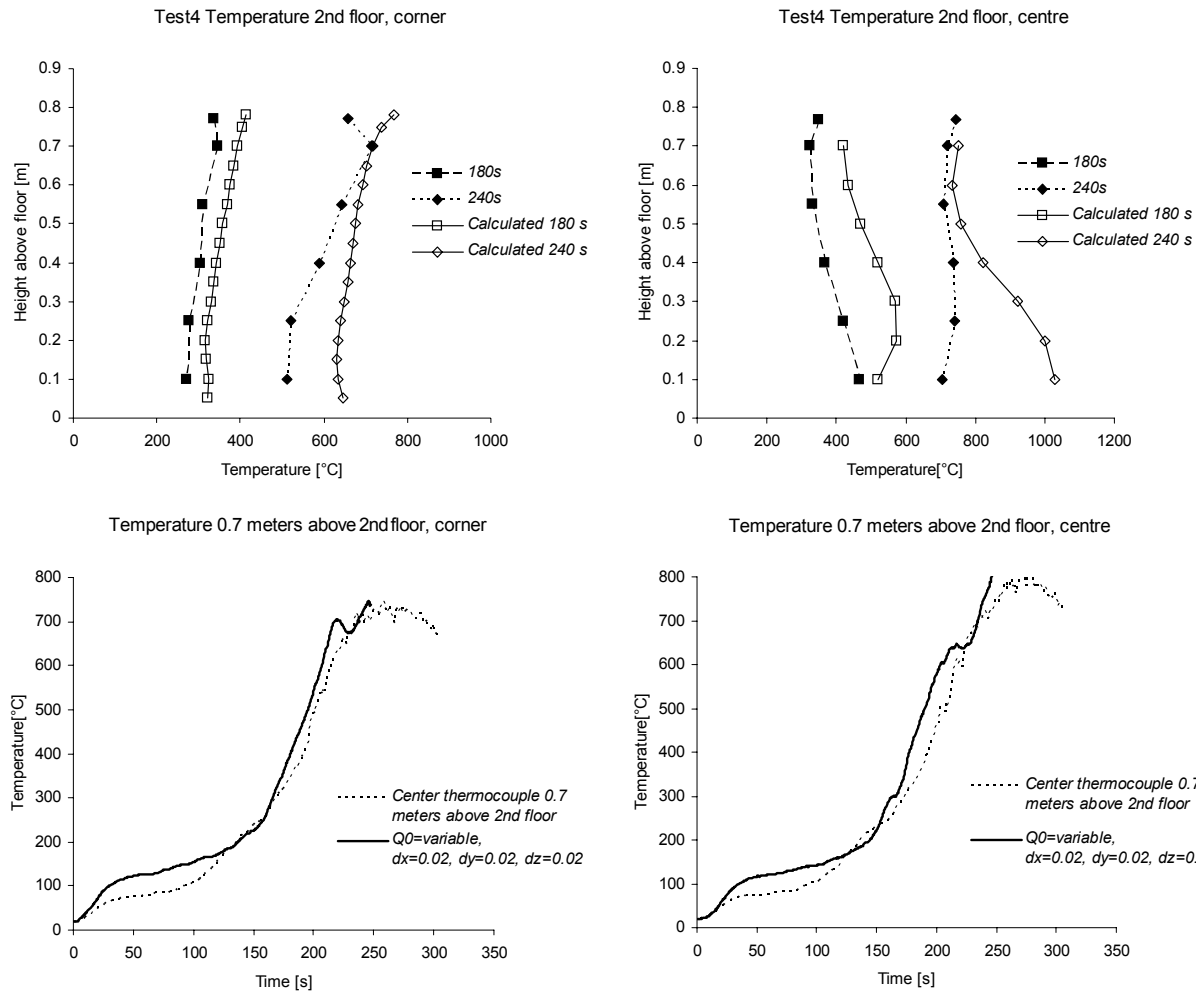

Figure 28. Comparison between predicted and measured gas temperature at some selected points in time and space in the top compartment. Again, all the predictions refer to a simulation using a curve-fitted initial fire and with the computational domain meshed according to a cubical form control volumes with 0.02 meter side.

Figure 30 provides further explanation to the overpredicted rate of fire growth and flame spread showing that the heat flux (here exemplified using the radiative heat exposure) to the floor, and consequently to all the surrounding walls, shows an increase, diverging from the experimental data after about three minutes after initiation of the initial fire. Since the measurement device (Gunners type radiation heat flux meter) measure the flux to a water cooled surface the simulation results shown in Figure 30 have been modified accordingly.

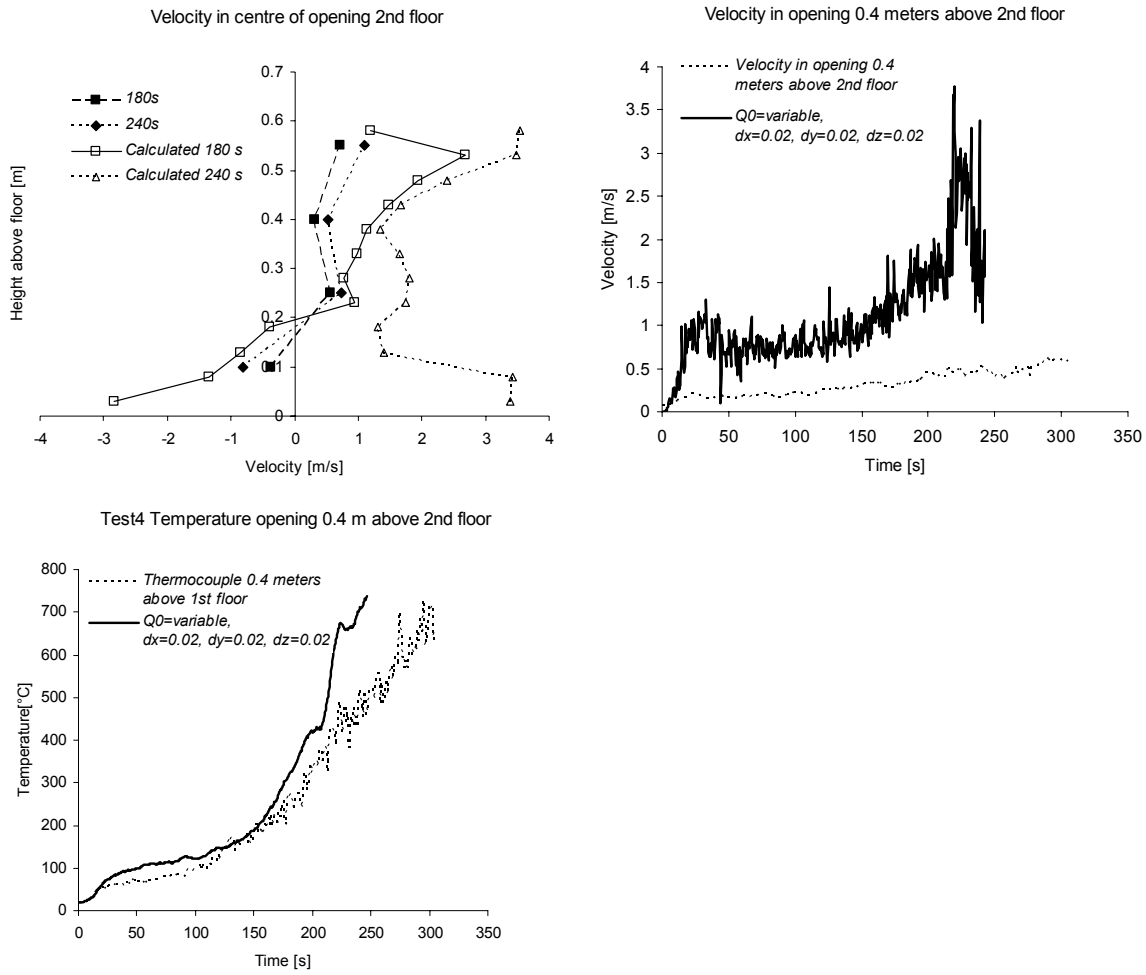

Figure 29. Comparison between computed and measured conditions from test V4 in the opening between the upper compartment and the surroundings. Clearly, the mass balance obtained in the simulation is not analogous to the experimental result.

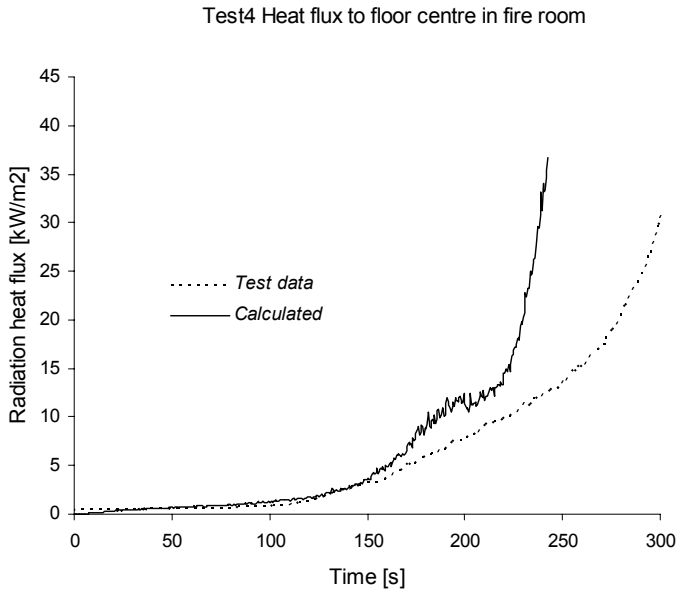

Figure 30. Radiation heat flux to floor in the fire room in the simulation using the curve-fitted initial fire.

In comparing the computational results from the scenario termed V5, the trend from Figure 26 still holds that is, the end-result, most noticeable the time to flashover, is very sensitive to the heat release rate of the initial fire source. The simulation using a constant, average, initial fire size indicate a time to flashover which is about half a minute less than the simulation using a initial fire, curve-fitted to the load cell data. In this scenario (V5) the opening in the fire compartment is the only connection to the surroundings.

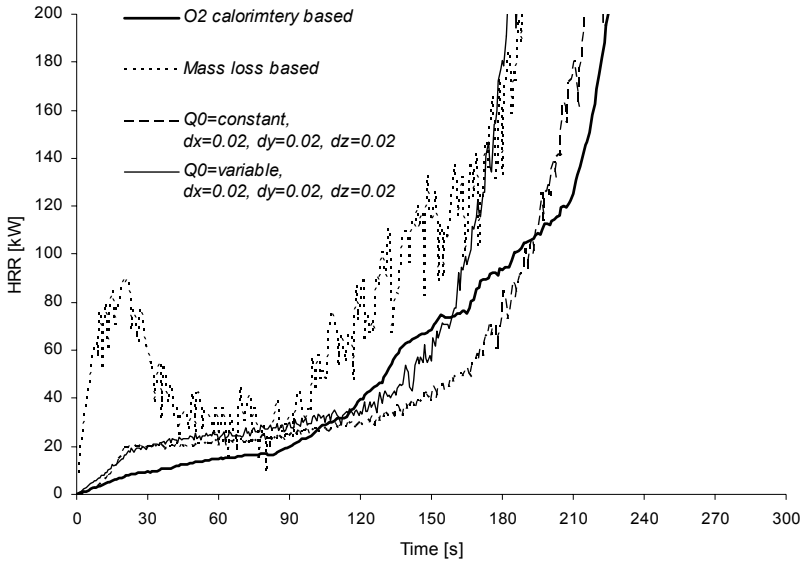

Figure 31. Total rate of heat release illustrating the fire growth and flame spread on the compartment walls, comparison of measurement data and calculated results for test V5.

Comparing the experimental data on gas velocity and temperature in the opening with the predictions as shown in Figure 32 it is obvious that the simulation is shifted in time, overpredicting the thermal effects and consequently the fire growth rate. Regarding the radiative flux to the floor, the computed results overpredict the level of exposure after about three minutes into the test, Figure 33. Clearly, a small overprediction of the incident heat flux will lead to a higher rate of pyrolysis which in turn leads to flame spread and subsequent fire growth further adding to the thermal exposure of the combustible linings. The flashover is predicted sooner than it occurred in the test, the growth rate however, is predicted with a high level of accuracy.

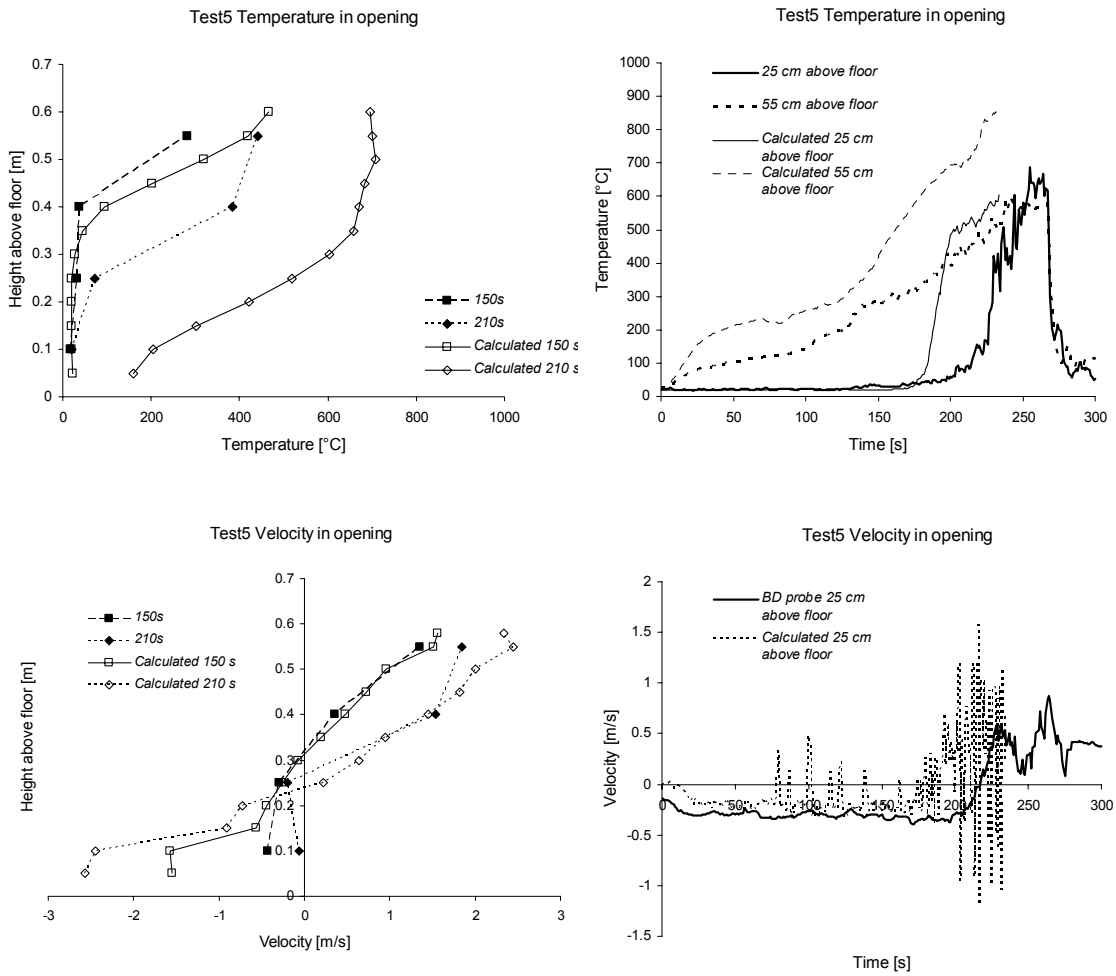

Figure 32. Gas temperature and velocity in the opening centreline. The predicted results are dislocated in time however, the trend is quite good.

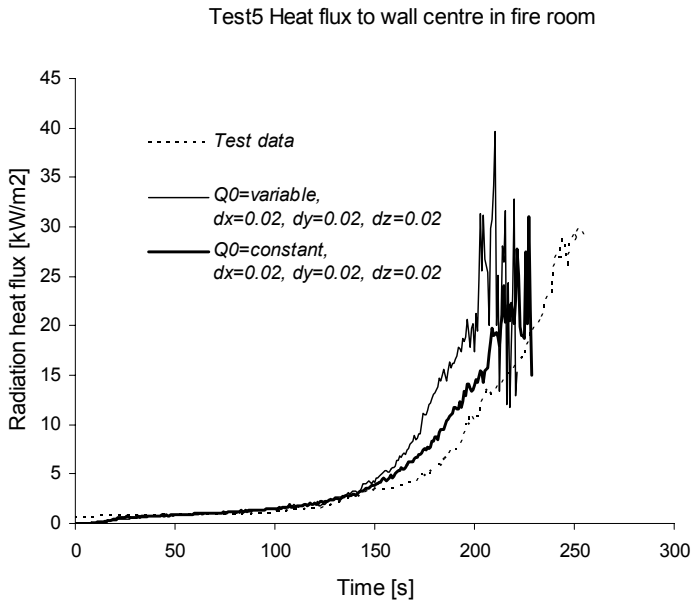

Figure 33. Comparison between experimental and computed radiative heat flux.

7.3 Two compartments in a horizontal array

Existing experimental data from two tests, using equal openings between the inner room (the origin of fire) and the outer room but with different ventilation openings between the outer room and the surroundings has been compared with computations. The venting conditions are summed up in Table 4. In the inner room the rear wall and both side walls were lined with a MDF board and the outer room has a MDF board attached to one of its side walls. The initial fire source was a heptane pool fire, although in the simulations no distinction was made between the combustible linings and the initial fuel source and thus the reaction for a cellulose-based material was used.

Table 4. Ventilation conditions in the scenarios being studied in this section.

Vent condition	**H1 (W×H)**	**H2 (W×H)**
Door opening; outer compartment	0.3×0.6	0.3×0.3
Opening between compartments	0.3×0.6	0.3×0.6

Heat release predictions and experimental data for the different tests are compared in Figure 34. The evaluations of the experimental data using different techniques show a great scattering, a phenomenon which is believed to be caused by the fire becoming underventilated in which case pyrolysis occurs but without the combustible gases being fully combusted.

The outcome of the simulation was found to be very sensitive to the description of the initial fire source. Considering Figure 34 (b) showing the heat release rate in scenario H2 a slightly different initial HRR results in fundamentally different predictions where the one approach suggest flashover after about 4-5 minutes while the other indicate no flashover at all (which was also the test result). The H2 scenario will not be addressed further in this report.

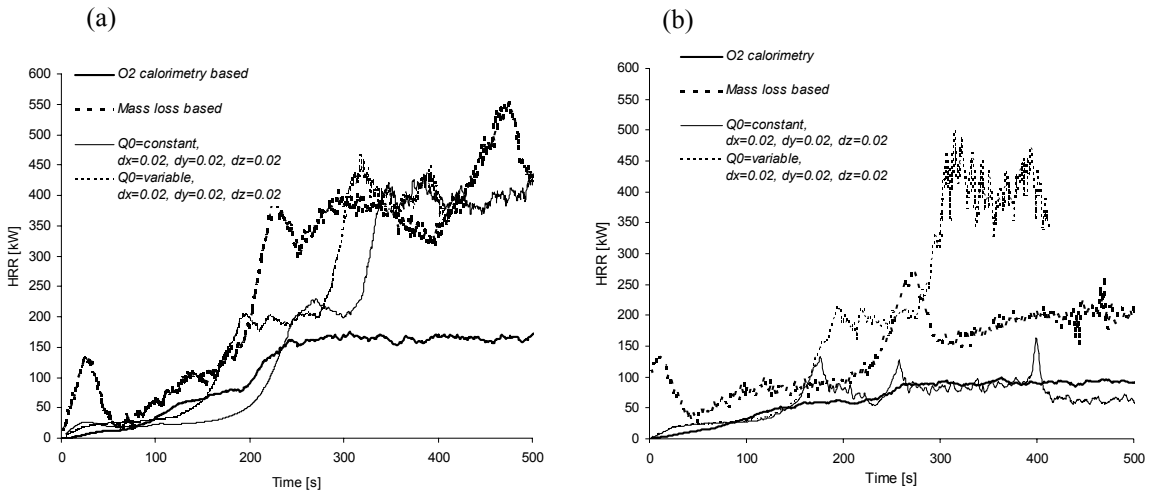

Figure 34. Comparison between computed and measured heat release rate using different techniques, (a) refers to test H1 and (b) to test H2 as described in Table 4.

In these scenarios the comparison between experimental data and the computational results show the importance of different modes of ignition and flame spread. Considering the simulation of scenario H1, using a curve-fitted initial fire growth, the result suggest that the fire in the inner room becomes underventilated after about three minutes, see Figure 35, after which combustion predominantly takes place in the opening and a distance into the fire room as fresh air is entrained into the opening. The heat release graph indicates that the fire has stopped growing, the rate of combustion is governed by the amount of air being mixed with the hot fuel gases. Four minutes after ignition of the initial fire the combustible lining in the outer room is ignited, apparently without direct flame impingement. One minute later the room reaches a state of flashover, the whole wall is burning.

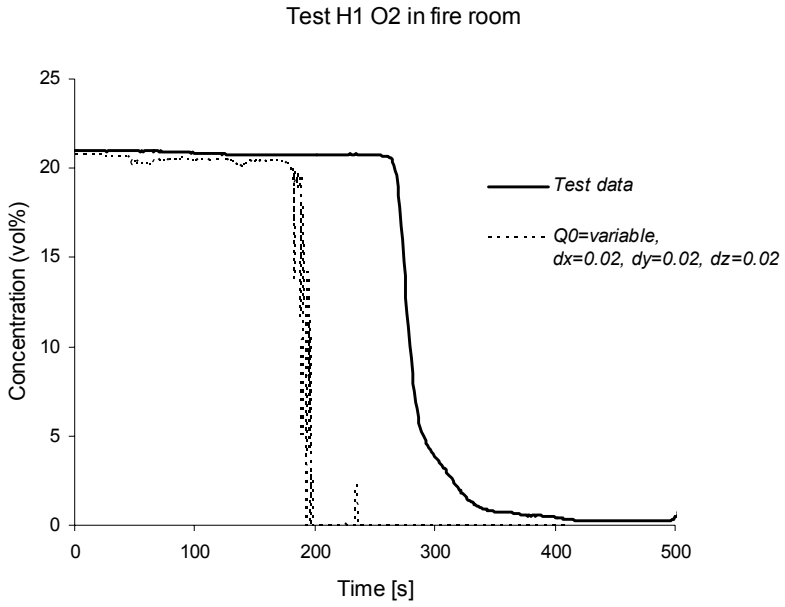

Figure 35. Oxygen concentration (by volume) in the inner room, the origin of fire.

In Figure 36 the computed temperature-time history at two locations in the fire room are presented and compared with thermocouple measurements, the locations being the front corner and centre of the room respectively. Although overestimating the initial gas temperature the computational results would generally be considered as being quite satisfactory. The end temperatures are predicted with a high level of accuracy as compared with the measurements.

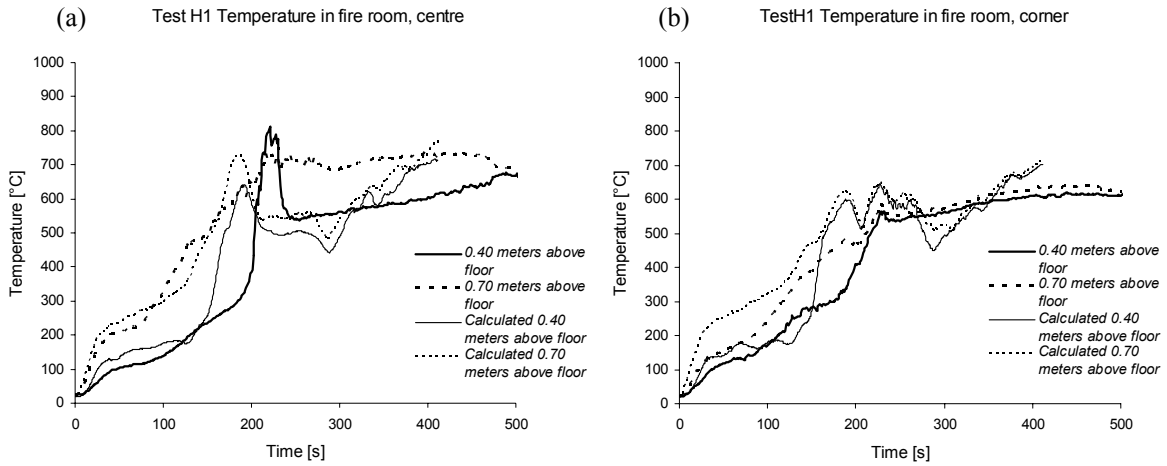

Figure 36. Comparison between computed and measured temperatures at two different locations in the room and at two different heights above the floor.

Considering the conditions in the outer room however, the simulation seem less satisfactory. Figure 37 compares measured and calculated gas temperature and velocity in the opening. While in these diagrams the velocity predictions shows great agreement with the BD probe measurements the temperatures have been overpredicted effectively making both mass- and energy balance over the opening incorrect.

To sum up, the simulation presents reasonable agreement with the experimental data on the conditions in the fire room. The predictions from the adjacent room show excellent agreement with measurements during the first 2.5 minutes after which the results seem to overpredict the thermal impact. This could be expected since the pyrolysis model presumes flame spread to be described as the continuous movement of a pyrolysis front initiated from piloted ignition, which is true in the inner room but is unlikely to be the case in the fire spread to the outer room, effectively resulting in the simulation overpredicting the rate of fire spread.

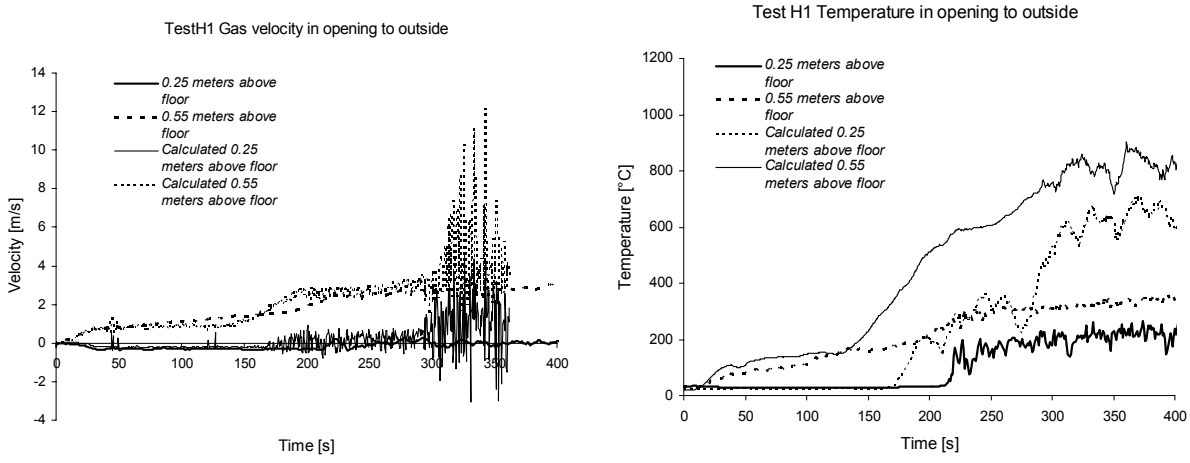

Figure 37. Comparison between measured and predicted gas velocity and temperature in the centre of the opening to outside.

As was described above, the simulation suggests the outer room to reach flashover after about four to five minutes of testing. This is further evidenced by Figure 38 showing the gas temperature to be greatly overpredicted in the later stages of the scenario.

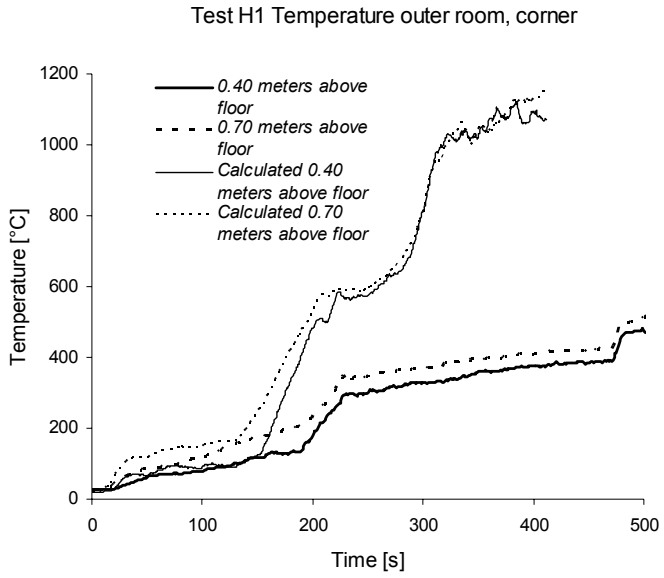

Figure 38. Temperature prediction in the front corner of the outer room compared with thermocouple measurements.

7.4 A note on flashover

The point in time when the flames reaches the ceiling may be a good indication of a forthcoming flashover. As the flames spreads out under the ceiling, the heat flux to nearby combustible materials increase promoting the fire spread and growth. A traditional definition of the term "flashover" used within different combustion related disciplines include the complete involvement of all combustible surfaces within the system. For example the ISO[32] definition of flashover: "The rapid transition to a state of total surface involvement in a fire of combustible materials within an enclosure". A standard enclosure fire grows with a fairly moderate rate and it may be more reasonable to apply a definition involving a time interval rather than a fix point in time, for example starting at the point in the HRR-time chart where the process of fire growth seem to run-away and ending with the total involvement of all combustibles in the compartment. One such definition is that of Chitty[33]: "During a compartment fire there can come a stage where the thermal radiation from the fire, the hot gases and the heated walls cause all combustible materials in the fire room to ignite. This sudden and sustained transition of a growing fire to a fully developed fire is called flashover".

A frequently used approximation in estimating the occurrence of flashover in enclosure fire experiments is to assume the equivalence between the inception of flashover with the

presence flames projecting out from the opening. This method was used when evaluating the video recordings from the tests simulated here[3]. In Figure 39 the measurements and observations from the tests in the single compartment are compared with estimations using the well-known expression of McCaffrey, Quintiere, and Harkleroad, MQH[34], based on the conservation of energy in the hot combustion gases. Evaluating for the rate of heat release, their equation is written as

$$\dot{Q} = h_{eff} A_T A_v H_v^{1/2} \left[\rho_0 c_p T_0^2 g^{1/2} \left(\frac{\Delta T_g}{480} \right)^3 \right]^{1/2} \quad \text{Eq. 13}$$

Where

h_{eff} = Effective heat transfer coefficient [$Wm^{-1}K^{-1}$]
A_T = Total surface area of the inner walls [m^2]
A_v = Area of the opening [m^2]
H_v = Height of the opening [m]
ρ_0 = Density of the ambient air [kgm^{-3}]
c_p = Specific heat capacity [$Jkg^{-1}K^{-1}$]
T_0 = Ambient temperature [K]
g = Gravity constant, 9.8 [ms^{-2}]
ΔT_g = Temperature difference between hot combustion gases and ambient air [K]

If it can be assumed that the thermal wave has reached the unexposed side of the walls and reached a steady state, the effective heat transfer coefficient can be evaluated from:

$$h_{eff} = \frac{k}{\delta} \quad \text{Eq. 14}$$

Where k is the thermal conductivity and δ represent the thickness of the wall. However, it is not likely that a steady state has been reached, in fact the thermal penetration time can be approximated to about 5 to 6 minutes and a more appropriate calculation procedure would be that of Eq. 15 including the thermal inertia of the wall material and the exposure time, t.

$$h_{eff} = \frac{k\rho c_p}{t} \quad \text{Eq. 15}$$

Figure 39 can now be formed using the classical criteria of a temperature increase of about 500 °C often used to define a state of flashover in a compartment fire. The MQH correlation indicates flashover earlier than the visual observation based on flames projecting out from the

opening. Instead the results coincide with the reported observations of flaming combustion in the lower part of the gas layer which clearly indicate that it is only a matter of time before all combustibles in the room have been ignited.

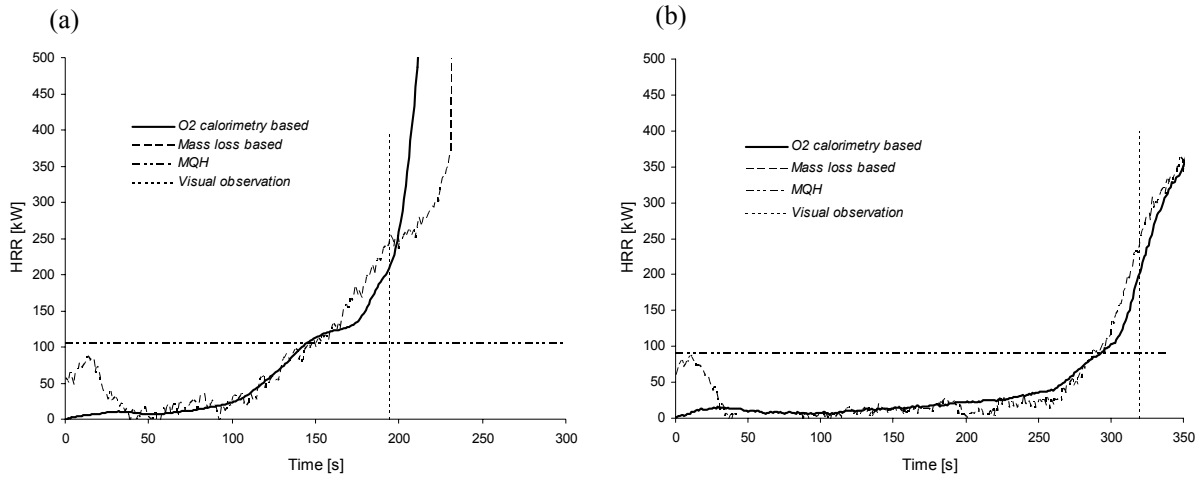

Figure 39. Applying the MQH relationship to approximate the time to reach flashover in the single compartment tests using heptane (a) and wood cribs (b) as the initial fire source

Similar analyses for the tests with two rooms in series are presented in Figure 40. The opening area in the MQH equation has been evaluated as an effective area according to Eq. 16,

$$A_{0,eff} = \frac{A_1 A_2}{\sqrt{A_1^2 + A_2^2}} \qquad \text{Eq. 16}$$

where A_1 and A_2 represent the openings between the rooms and between the outer room and the surroundings respectively.

Since no documentation on the time to flashover in the inner compartments are available from visual observations, the time to reach 550 °C are used to indicate a state of flashover.

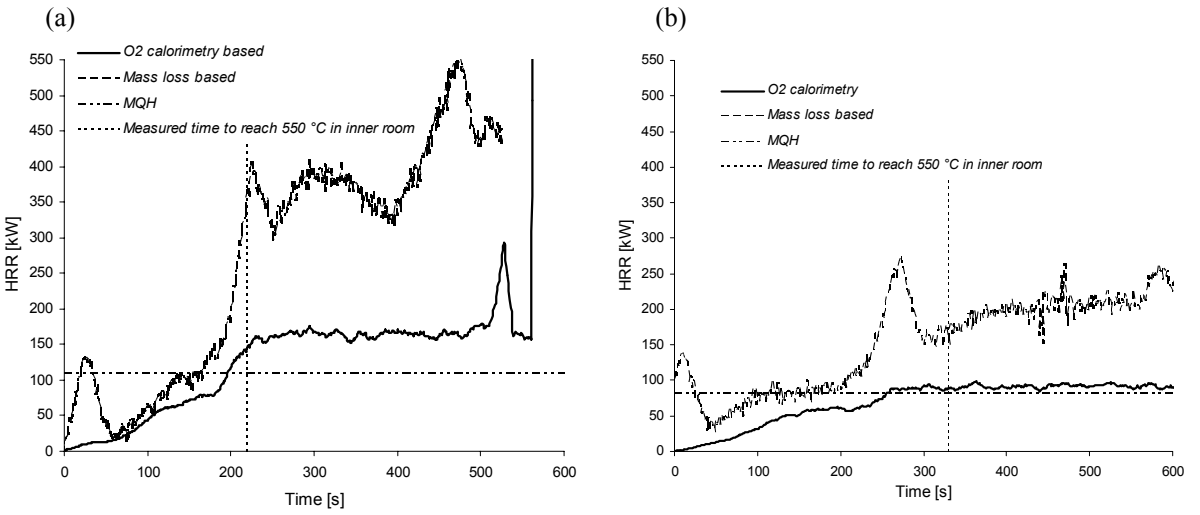

Figure 40. Comparison between the MQH equation and measurements from tests H1 (a) and H2 (b).

8. Conclusions and recommendations

The development of the pyrolysis model used by the FDS code is based upon the consideration of heat transport into a combustible material. The subsequent thermal response of the material is modelled using a single-step Arrhenius rate law of the first order. While this methodology is likely to be the most reasonable in terms of physical modelling, in terms of practical modelling it has a major drawback in the lack of credible input data, the suggestions found in the literature often showing a variation by several orders of magnitude. Thus, in order to obtain the, material dependent, set of input data that works well with the model one is referred to the use of a trial and error approach, using the model in a stand-alone mode and comparing the outcome with results from some kind of small-scale experimental set-up. Despite the weaknesses of the Cone Calorimeter apparatus, several factors works to favour its use, the availability and the large number of testing labs offering this kind of analysis and the amount of data already being published to name a few.

In order to have a minimum of unknown parameters when comparing the model performance with the mass loss rate (or rate of heat release) from Cone Calorimeter testing, the thermal properties of the combustible material were determined in advance using surface temperature measurements when the material was exposed to different heat fluxes. The parameters were derived using both 1-D and 3-D analysis thus providing an estimation of the importance of 3-D effects.

Some of the comparisons between experimental data and the computational results indicated very good predictive capabilities. This was rather unexpected since the code makes some substantial simplifications in, for example, the modelling of combustion, radiation and boundary layer flows. In comparing different grid options however, a node independent solution could not be found. Nevertheless, the first choice of meshing, using cubical control volumes with a side length of 0.1 times the characteristic diameter of the initial fire, consistently showed to be the best choice. An interesting assignment could be to evaluate this in other scenarios to check on the extrapolative potential. For example, a simulation of the Room Corner test (using a 100 kW initial fire) should then have a cubical grid with a side length of 0.04 meter.

From the CFD analysis presented in this report it is clear that the description of the initial fire source is a decisive parameter in the simulations of flame spread and fire growth. In a fire design situation, no such information is available and thus the end-result will be rather random, depending strongly on the initial fire as chosen by the engineer responsible for the analysis.

Furthermore, the pyrolysis model and the input data that were used in this work are originally intended for the simulation of flame spread situation that can be described as the subsequent piloted ignition along a continuous combustible surface. A scenario including sustained spontaneous ignition, for example due to hot gases flowing past a combustible solid or thermal radiation from a hot gas layer in the absence of flames, is quite another problem. Using the same input data for these scenarios may result in an incorrectly predicted time to ignition and, because of the lower degree of preheating, a wrongly predicted fire growth rate.

In the comparison with experimental data the predictions generally shows good agreement during the initial growth phase on the combustible linings. The computational results of the later stages however, are not as coherent. No node independence could be shown but the cubical control volumes with side length 0.02 meters, as derived from the dimensionless diameter of the initial fuel source, showed consistent predictions. Nevertheless further studies need to be made until general advice can be given and strictly speaking the node dependence shown in the simulations should not be accepted. Further development of heat transfer models are required in order to make use of the material models that has been available for a long time. Furthermore, there is an urgent need of consistent material data compatible with the modelling efforts being made.

Although perhaps one of the most sophisticated pyrolysis models implemented into a CFD code that exist today, it may be that the simulation of the flow as well as the simplifying assumptions being made in the derivation and implementation of the model, such as the use of a single step rate law and the omission of momentum equation, act to restrain its capabilities. The simulation of a turbulent reacting flow is extremely complex and the accuracy required for the pyrolysis models for successful flame spread simulations cannot be satisfied using the simplifications on soot fraction, radiation and convective heat flux that are used with success in simulations of the smoke movement in enclosures.

The semi-empirical relationship of McCaffrey, Quintiere and Harkleroad was shown to be useful in predicting the time to flashover.

References

1 Walmerdahl P., Piloted Ignition of Materials – An introductory experimental study on wooden material, FOI MEMO 01-4249, Grindsjön research centre, 2001.

2 Walmerdahl P., Spontaneous and Piloted Ignition of of Materials – An experimental study on MDF board, FOI MEMO 02-2485, Grindsjön research centre, 2002.

3. Walmerdahl P., Werling P., Fire Growth and Spread – An experimental study in model-scale, FOI-R-0907--SE, Grindsjön, 2003.

4 Carlsson J., Computational Strategies in Flame-Spread Modelling Involving Wooden Surfaces - An evaluation study, Dept Fire Safety Engineering, Lund University, Lund, 2003.

5 ISO 5660, Fire Tests – Reaction to Fire – Rate of Heat release from Building Products, International Standards Organisation, Geneva, 1991.

6 de Ris J., Spread of Laminar Diffusion Flame, 12th Symposium (International) on Combustion, The Combustion Institute, 1969.

7 Williams F. A., Mechanisms of Flame Spread, 16th Symposium (International) on Combustion, The Combustion Institute, 1976.

8 Karlsson B., Thomas P, On Upward Flame Spread On Thick Fuels, SE-LUTVDG/TVBB-3058, Lund University, Lund, 1990

9 Saito K., Quintiere J G., Williams F A., Upward Turbulent Flame Spread, Proceedings from the First International Symposium on Fire Safety Science, Hemisphere Publishing, New York, 1984.

10 Karlsson B., Modelling Fire Growth On Combustible Lining Materials, PhD Thesis, Lund University, Lund, 1992.

11 Yan Z., Numerical Modelling of Turbulent Combustion and Flame Spread, PhD Thesis, Lund University, Lund, 1999.

12 Hostikka S., McGrattan K., Large Eddy Simulation of Wood Combustion, Proceedings of the 9th Interflam Conference, Edinburgh, 2001.

13 Atreya A, Pyrolysis, Ignition and Fire Spread on Horisontal Surfaces of Wood, Division of Applied Sciences, Harvard University, Cambridge MA, 1984.

14 The CECOST Home Page, http://www.cecost.lth.se/, 2004.

15 Babrauskas V., The Cone Calorimeter, Heat Release in Fires, Editors: Babrauskas V., Grayson S. J., Elsevier Applied Science, ISBN 1-85166-794-6, 1992.

16 Nussbaum R. M., B. A.-L. Östman, Larger Specimens for Determining Rate of Heat Release in the Cone Calorimeter, Fire and Materials, vol. 10, No. 3 & 4, pp 151-160, 1986.

17 Babrauskas V., On the Rate of Heat Release in the Cone Calorimeter, Letter to the Editor, Fire and Materials, vol 11, No. 4, p 204, 1987.

18 Moghtaderi B., Combustion Characteristics of Solid Fuels Under Fire Conditions, PhD thesis, Department of Mechanical and Mechatronic Engineering, The University of Sidney, Australia, 1996.

19 Tsantaridis L., Reaction to Fire Performance of Wood and Other Building Products – Cone Calorimeter results and analysis, PhD Thesis, KTH Royal Institute of Technology, Stockholm 2003.

20 Andersson P., Blomqvist J., Smoke Detection in Buildings with High Ceilings, Brandforsk project No 628-011, SP-report 2003-33, Borås, 2003.

21 William D. D., Notarianni K A., McGrattan K. B., Comparison of Fire Model Predictions with Experiments Conducted in a Hangar with 15 meter Ceiling, NISTIR 5927, BFRL, NIST, Gaithersburg 1996.

22 Hostikka S., Keski-Rahkonen O., Results of CIB W14 Round Robin for Code Assessment Scenario B. Draft 31/08/98, VTT Technical Research Centre of Finland, 1998.

23 Grandison A.J,.Galea E.R., Patel M.K., Fire modelling standards/benchmark - Report on Phase 1 Simulations, Fire Safety Engineering Group, University of Greenwich, London, 2001.

24 Patankar S. V., Numerical Heat Transfer and Fluid Flow, Series in computational methods in mechanics and thermal science, Taylor & Francis, ISBN 0-89116-522-3, 1980.

25 Versteeg H. K., Malalasekera W., An Introduction to Computational Fluid Dynamics – The Finite Volume Method, Longman Group Ltd, ISBN 0-582-21884-5, 1995.

26 Wilcox, D. C., Turbulence Modelling in CFD, DCW Industries Inc, 2001.

27 McGrattan K. B., et al., Fire Dynamics Simulator (Version 2) – Technical Reference Guide, National Institute of Standards and Technology, NISTIR 6783, 2001.

28 LeVan, Susan L. Thermal Degradation, Schniewind, Arno P., ed. Concise Encyclopedia of Wood and Wood-Based Materials. 1st edition. Elmsford, NY: Pergamon Press: 271-273. 1989.

29 Leckner B., Hansson K-M, Tullin C., Borodulya A. V., Dikalenko V. I., Palchonok G. I., Kinetics of fluidized bed combustion of wood pellets, Proceedings of the 15th International Conference on Fluidized Bed Combustion, Savannah, Georgia, May 16-19, 1999.

30 NIST homepage, http://fire.nist.gov, 2004.

31 Göransson U., Omrane A., Surface temperature measurements in the cone calorimeter using phosphorescence, Proceedings of the 10th Interflam Conference, Edinburgh, 2004.

32 ISO/IEC Guide 52, Glossary of Fire Terms and Definitions, International Standards Organisations, 1990.

33 Chitty, R., A survey of backdraft, Fire Research and Development group, Home Office, 1994.

34 McCaffrey B. J., Quintiere J: G. and Harkleroad M. F., Estimating Room Fire Temperatures and the Likelihood of Flashover Using Fire Test Data Correlations, Fire Technology, Vol 17, No 2, 1981.